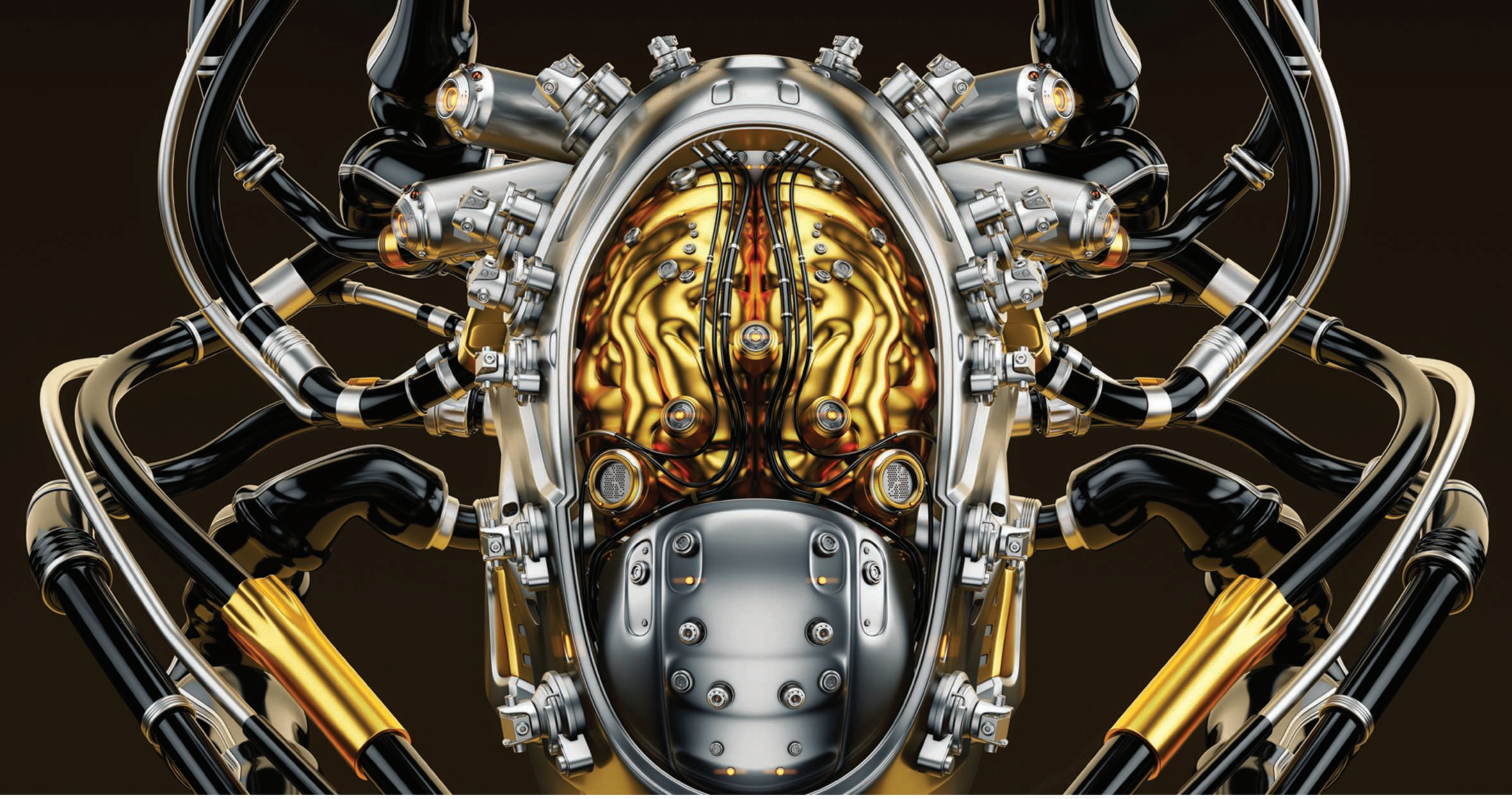

A Review of Cable-Driven Parallel Robots

Typical Configurations, Analysis Techniques, and Control Methods

By Mahmoud Zarebidoki, Jaspreet Singh Dhupia, and Weiliang Xu

Cable-driven parallel robots (CDPRs) have applications in large workspaces and at high operating speeds, which necessitates considering the mass and elasticity of cables for accurate analyses of kinematics, dynamics, workspace, trajectory planning, and control. In this article, first, the typical CDPR configurations along with their application areas are summarized. Then, various approaches, such as optimizing cable and motor configurations or integrating additional elements to the structure of CDPRs that can be used for workspace geometry optimization, are discussed. Afterward, different models for the cables with mass and elasticity, such as Irvine's sagging or spring dampers studied in the literature for integrating into the kinematics and dynamics equations, are reported. Later, along with reviewing different approaches for trajectory planning of planar and spatial CDPRs, advances in configuration optimization for collision-free trajectory planning are addressed. Finally, kinematic and dynamic control algorithms to handle the effect of mass and elasticity of the cables and robust and adaptive control algorithms to tackle structured and unstructured uncertainties, such as in the mass and moment of the moving platform (MP) and external disturbances, are reported.

Digital Object Identifier 10.1109/MRA.2021.3138387
Date of current version: 29 March 2022

Background

Flexible cables are used instead of rigid links in CDPRs for connecting the base platform (BP) to the MP. In these robots, cables are wound or unwound using electrical motors, winches, and pulleys to move the MP. CDPRs have several advantages over conventional link-based robots because of their ability to generate higher velocities and accelerations because of a lower inertia, large workspace, and a high load capacity [1], [2]. The initial ideas on cable-controlled robotic systems originate from a master thesis [3] in 1984. SkyCam [4] and RoboCrane [5] are considered the first applied robots of this kind, developed in the 1980s to carry a recording camera and to perform a pick-and-place task, respectively. In the 1990s, the first research about the problem of tension distribution of cables was studied in [6], where adding additional cables for constraining the MP was proven. The first classification of CDPRs based on the number of cables and degrees of freedom (DoF) was introduced in [7]. By the turn of the century, along with a broadened research about CDPRs in academics, their practicality in the industry in applications to different tasks, such as pick and place, rehabilitation, and 3D printing, was proven.

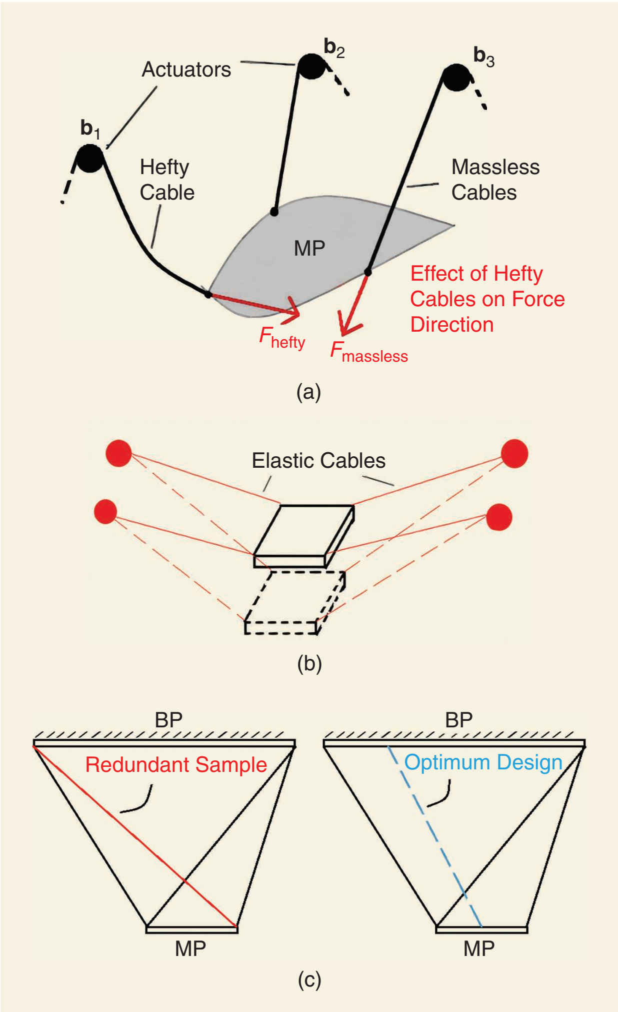

Figure 1. (a) Hefty cables with mass and their effect on the kinematics and dynamics. (b) Effect of elasticity of cables in CDPRs. (c) Minimum-time trajectory optimization by changing the cable configuration, adapted from [50].

Different characteristics of cables, such as material, density, and elasticity, can influence the static and dynamic behavior of a CDPR [2]. Among these characteristics, the effect of the mass and elasticity of cables on CDPR performance is often studied in the literature for accurate robot analysis. The mass of a cable can be ignored if its tension is considerably greater than its weight [8]. However, a large cable mass is required in applications with a large workspace, which cannot be ignored in the kinematics and dynamics formulation [9]–[20]. For example, a Five-hundred-meter Aperture Spherical radio Telescope (FAST) was designed in China; it is the largest single-dish radio telescope in the world. The feed cabin of this mechanism is supported and driven by cables within a reflector with a curvature of radius 300 m [21]. Other examples of large-workspace CDPRs are MARIONET-CRANE [22] and COGIRO [11], which were developed for handling and assembling heavy parts within the workspace dimensions of 15 m × 15 m × 15 m and 15 m × 11 m × 6 m, respectively. These applications need a large workspace, so the modeling of cables with mass [Figure 1(a)] should be integrated into the kinematics and dynamics equations. The elasticity of a cable can strongly affect the performance and efficiency of a CDPR, especially for applications with a higher speed [18], [23], [25]–[29].

In 1995, it was shown experimentally that CDPRs can generate accelerations of more than 400 m/s^2 [2]. Later, a high-speed spatial CDPR was introduced in [1] capable of accelerating up to 43 g and a maximum speed of 13 m/s. In such applications, it is necessary to consider the elasticity of cables and its effect on resulting displacements and vibration during the formulation of the kinematics and dynamics of the system [Figure 1(b)]. Therefore, the cable models used in the literature consider 1) cables with no mass and no elasticity; 2) elastic cables with no mass; 3) cables with mass and no elasticity, assuming them to have a straight line or hefty contours; or 4) cables with both mass and elasticity.

Incorporating a lightweight structure and its modularity makes CDPRs more reconfigurable and scalable than traditional rigid robots. Various cable and motor configurations are studied in the literature to describe frameworks for optimal trajectory planning [30]–[33] and optimal workspace generation [30], [34]–[46]. Moreover, the cables can wrap around obstacles [33] or collide with each other in a cluttered environment. Therefore, [30] and [34] have considered changing the configuration by changing the connection point to the BP or MP [Figure 1(c)] to avoid collisions in the approaching phases.

Compared to previous literature reviews [47], [48] on cable-driven robots, this article covers research that considers the mass and elasticity of cables for subsequent analysis and configuration optimization of CDPRs in more detail.

Common CDPR Design Configurations and Applications

CDPRs can be categorized into different types based on their configuration, the number of cables, and the DoF. A

CDPR with M cables and N DoF is an incompletely restrained positioning mechanism (IRPM), if $M \leq N$. For such a configuration, the robot cannot resist arbitrary applied wrenches. However, considering gravity or other applied forces, one or more poses of an IRPM may exist where the robot is in stable or unstable equilibrium. If $M = N + 1$, the robot can be a completely restrained positioning mechanism (CRPM) in certain poses. In this case, possible tension distributions form a 1D subspace in the M-dimensional space of cable forces, making it comparably simple to solve. If $M > N + 1$, the robot is a redundantly restrained positioning mechanism (RRPM). In this case, based on the robot configuration, there might be infinitely many solutions for the tension distribution in the cables; therefore, two significant problems should be solved. The first is to find out if there is at least one solution for tension distribution; the second, if there are many solutions, is how to find continuous smooth ones along a trajectory [2], [51].

Different configurations of CDPRs consisting of IRPMs, CRPMs, and RRPMs can operate in a suspended configuration where the robot relies on gravity to be balanced. In this case, suspended CRPMs and RRPMs will have the maximum of N cables under tension [52]. This issue makes notable differences in a CDPR's analysis as all slack cables should be ignored.

Different typical configurations of CDPRs are illustrated in Figure 2, and typical applications corresponding to different configurations of CDPRs are presented in Table 1. The following sections discuss different research aspects of IRPMs, CRPMs, and RRPMs involving kinematics, dynamics, workspace, trajectory planning, and control.

In addition to the basic architecture of CDPRs, other configurations were also proposed in the literature by replacing some of the cables with other elements, such as rigid links, revolute joints, springs, and extension limbs. In [53] and [54], a telescopic spine and an extensible limb provide appropriate pressure to the MP to maintain all of the cables in tension. The force and torque capacity of the MP can be modified by applying the required ballast force. On the other hand, the robot's reachable workspace decreases as these elements' length and swing angle are limited. In [55], a cable-driven mechanism with Cartesian motion was introduced. The robot consists of a rigid-link Cartesian mechanism that is driven with a cable loop with stationary actuators. Springs have also been integrated into the structure of CDPRs for constraining the robot without adding extra cables and actuators [56] or for optimizing and enhancing the required workspace [44], [45].

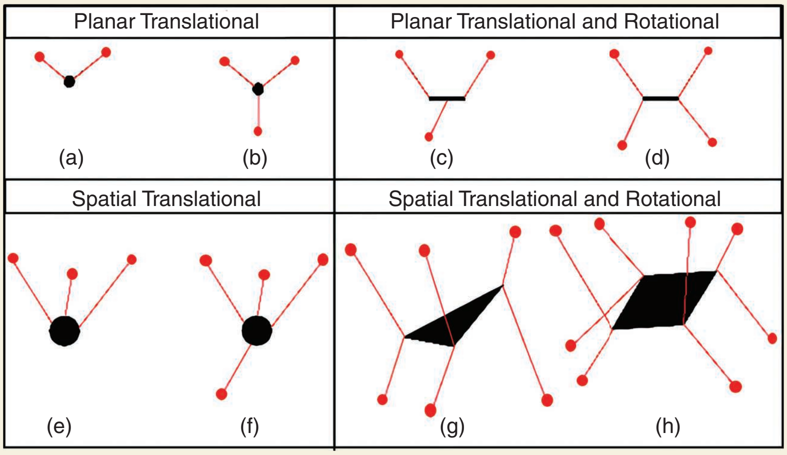

Figure 2. Different types of CDPRs: (a) 2–2 planar IRPM, (b) 3–2 planar CRPM, (c) 3–3 planar IRPM, (d) 4–3 planar CRPM, (e) 3–3 spatial IRPM, (f) 4–3 spatial CRPM, (g) 6–6 spatial IRPM, and (h) 8–6 spatial RRPM [57].

Kinematics and Dynamics

In this section, research on the kinematics and dynamics of CDPRs considering and not considering the mass and elasticity of the cables are reviewed. Compared to serial robots,

Table 1. Typical applications with corresponding CDPR configurations.

Application	Type	References
Pick and place	Planar CRPM	[140]
	Spatial IRPM	[5], [34], [64], [65], [68], [118], [135]
Simulator	Spatial CRPM	[26], [27], [103]
Radio telescope	Spatial IRPM	[21], [88], [137]
Rehabilitation	Planar CRPM	[94], [109], [110], [124], [144]–[152]
	Spatial IRPM	[109], [125], [153]–[155]
3D printing	Spatial IRPM	[156], [157]
	Spatial CRPM	[158]–[161]
Camera carrier, Inspection, and so on	Planar CRPM	[162], [163]
	Spatial IRPM	[4], [98], [104], [108], [164], [165]
Painting and so on	Planar IRPM	[78], [92], [93], [166], [167]
	Spatial RRPM	[168]
Logistics	Spatial RRPM	[143], [169], [170]
Maritime	Spatial IRPM	[172], [173]
Aerial	Spatial IRPM	[174]–[177]
	Spatial RRPM	[178]
Joystick	Spatial IRPM	[24], [171], [179]

the forward kinematics (FK) for parallel robots is more complex to solve. It is even more difficult in the case of CDPRs because of the unilateral nature of cables, which requires them to always be in tension. Inverse kinematics (IK) is easier than the FK to solve for parallel robots and CDPRs with ideal cables with no mass and elasticity. Furthermore, the hefty shape of the cables makes the IK problem quite complex. In this case, both the position parameters and cable tensions are unknowns, and some of the equations are not algebraic. Therefore, approaches that are efficient with ideal cables cannot be used for IK analysis. By assuming a hefty elastic model for the cables, solving the IK problem becomes even more complex as the cable configuration considers both hefty shape and elongation of the tensioning cables [58]. The details about elastic and hefty cable models and their effect on the kinematics and dynamics are explained in the sections "Cables with Mass," "Research Works Considering Elastic Cables," and "Research Works Considering Cables With Both Mass and Elasticity."

A positive effect of the five-bar mechanism on decreasing the drive torques and increasing the load-carrying capacity of the robot was demonstrated.

Research Works Assuming Massless Inelastic Cables

The Newton–Euler method was widely used for deriving the dynamics equations of both planar and spatial CDPRs [5], [26], [59], [60]. In this approach, the position vector of each cable and applied forces and wrenches on the MP were calculated for deriving the dynamics equations. In [61], a new Jacobian matrix was constructed with a chosen set of variables arising from dynamics analysis using the Lagrangian method. The dynamics equation presented in [59] has six variables corresponding to the position and orientation coordinates for the six DoF of the MP. However, the new Jacobian matrix employed Cartesian coordinates of the vertices of the MP consisting of nine variables, which reduces the computation time for workspace definition. In [62], the FK was studied using the multilayer perception type neural network approach, which is faster than numerical approaches. A backpropagation procedure was utilized for training the network. In [63], an approach for finding the lowest stable equilibrium pose of suspended CDPRs with an arbitrary number of cables was studied. In this approach, the potential energy of MP is minimized using the branch-and-bound algorithm.

The kinematics of the collaborative transport of cable-suspended payloads by four mobile cranes was examined in [64]. The estimation of kinematic errors caused by machining, assembly, and operation was studied to improve the exact positioning of the MP. Moreover, in [65], an IK analysis of three quadrotors carrying a payload was presented. The IK problem has infinitely many solutions for this configuration. However, when the tensions of the cables are also specified, the IK problem is shown to have a finite number of solutions.

Different approaches are used in the literature to account for the effect of the winding mechanism for improving the dynamic performance of the CDPRs [66]. In [67], reflective pulleys were integrated into the MP to improve the kinematics and dynamics of the robot. These reflective pulleys must have the same radius as the ones at the BP to compensate for their impacts. However, according to [2], pulleys have a significant effect only on the kinematics of small CDPRs and can otherwise be neglected. In [68], a five-bar mechanism was used to move the MP of a spatial IRPM. A positive effect of the five-bar mechanism on decreasing the drive torques and increasing the load-carrying capacity of the robot was demonstrated. In [28] and [66], the dynamics of pulleys and winches were considered for deriving kinematics and dynamics equations of a spatial and a planar robot using geometrical approaches.

Cables With Mass

Two approaches have been proposed in the literature for analyzing the kinematics and dynamics of CDPRs, considering the mass of cables. The first approach assumes cables as straight elements, and the second one accounts for their hefty or catenary shape.

In terms of the first approach, in [14], the cables were assumed as straight lines with varying mass and velocity. Dynamics equations of a 4–3 planar IRPM were derived using the Lagrangian method. In [15], the virtual work and Newton–Euler methods were used to analyze the dynamics of the MPs and cables of the FAST, respectively. In [13], cables were modeled as cylinder elements. The motion analysis of a 7–6 CRPM was studied using the "bushing" joint of ADAMS software.

The second approach was applied in [19], where the cable configuration (Figure 3) is represented with a hyperbolic function,

$$y(x) = k \cosh\left(\frac{x}{k} + c_1\right) + c_2, \tag{1}$$

where $k = H/q$, q is the distributed mass of the cable, H is the horizontal tension force, and c_1 and c_2 are two constants that can be evaluated from the boundary conditions.

Dynamic equations were derived for a hefty configuration of the cables considering aerodynamic forces acting on the robot by discretizing the cable into a series of N elastic segments joined at nodes [9]. The lumped-mass method was used to develop partial differential equations, which were solved using the adaptive Runge–Kutta algorithm. In [10], besides considering the mass of cables, the dynamics of pulleys were integrated for kinetostatic analysis. In [16], (1) was simplified for statics analysis, where a linear relationship was derived between the forces in the cables and the externally applied wrench to the robot's MP. Finally, in [69], an interval-analysis-based algorithm was used to solve the direct geometric–static problem of spatial IRPMs. The algorithm finds all possible equilibrium poses of an MP considering slack in the cables along with its mass.

Research Works Considering Elastic Cables

Transversal vibrations of cables can be neglected relative to axial vibrations. In [29], the axial and transversal vibration of a 7–6 CDPR was studied. It was shown that the transversal vibration contributes only 1.4% of the total vibration amplitude. The nonlinear stiffness characteristic of a cable that was used for a CDPR is shown in Figure 4(a).

Cables are mostly modeled as axial springs [Figure 4(b)] for CDPRs with elastic cables. In this case, the elongation ΔL of a cable is calculated as $\Delta L = K_c T_c$, where K_c and T_c are the stiffness and the tension applied to a cable, respectively. The cable's stiffness can have linear or nonlinear behavior. However, most of the literature considers a linear stiffness, $K_c = EA/L$, where E is Young's modulus of the cable material, A is the cable cross-sectional area, and L is the cable length at rest.

In [70], the IK and FK of a 7–6 IRPM with elastic cables were presented under the assumption that the tensions must be lower than a fixed threshold to avoid breaking the cables. In [29], a vibration analysis of general 6-DoF CDPRs was presented. The natural frequencies of the multibody system were analyzed to demonstrate that a cable manipulator can be designed to be stiff enough for special applications. In [71], the Euler–Lagrange formulation was used to derive the dynamic equations by first calculating the kinetic and potential energy of the MP and elastic cables. In [72] and [73], the cables were considered straight elements with elasticity and a damping coefficient having an inverse relation with the cable length. The Euler–Lagrange formulation was used to derive the dynamics equation.

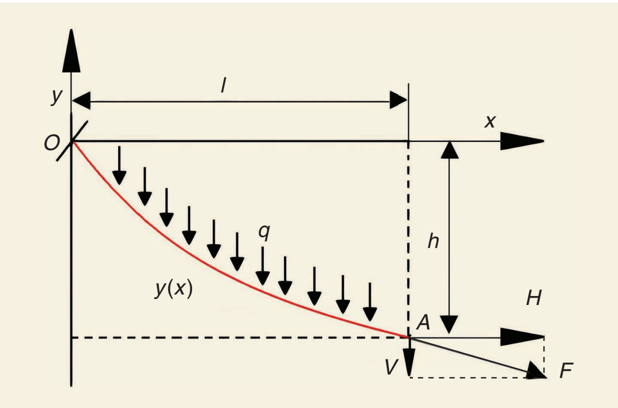

Figure 3. The catenary shape of cables considering the mass of the cables. (Source: [19]; used with permission.)

Research Works Considering Cables With Both Mass and Elasticity

The Irvine sagging-cable model [25], [74] is mostly used for deriving kinematic and dynamic equations considering both the mass and elasticity of cables. In this formulation, the ordinary differential equations for the coordinates of point A, which is the cable's connection point to the MP (Figure 3), are defined as

$$x_A = H\left(\frac{L}{EA} + \frac{\sinh^{-1} V - \sinh^{-1}\left(V - \frac{\rho g L}{H}\right)}{\rho g}\right), \tag{2}$$

$$y_A = \frac{\sqrt{H^2 + V^2} - \sqrt{H^2 + (V - \rho g L)^2}}{\rho g} + \frac{VL}{EA} - \frac{\rho g L^2}{2EA}, \tag{3}$$

where V is the horizontal tension force, and E, A, L, H, and ρ were described earlier in the sections "Cables with Mass" and "Research Works Considering Elastic Cables."

This model was used for setting up the cable configuration in [17] and [19], where the dynamics and kinematics modeling of the FAST was derived. The kinematic and force singularities were analyzed to improve the real-time controllability of the system. In [24], the static displacement of cables was computed and used for IK analysis and stiffness of general

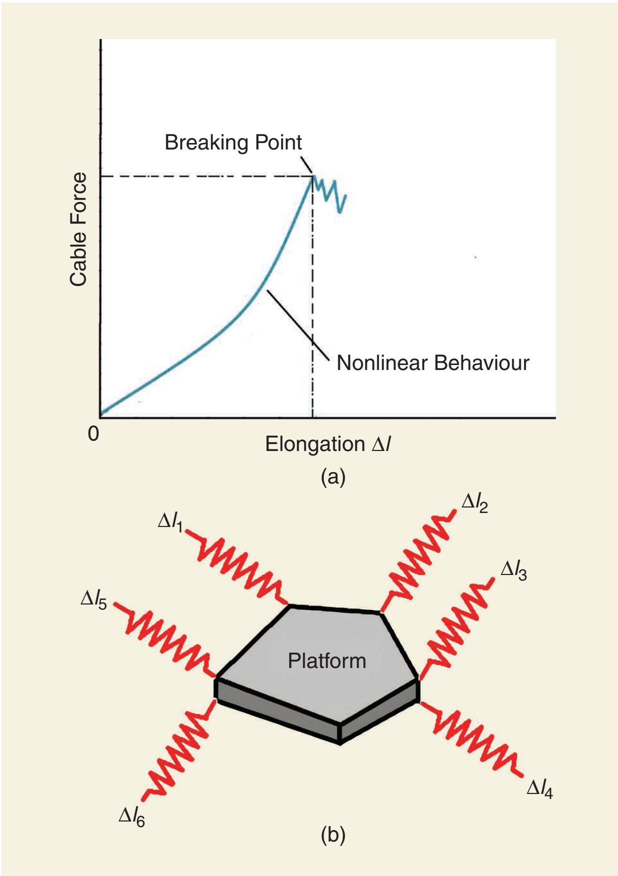

Figure 4. (a) The nonlinear behavior of a cable used for a CDPR and (b) elastic cables considered as linear springs for kinematics and dynamics analyses.

CDPRs. In [25], the FK of spatial IRPMs was solved using a numerical continuation scheme. The FK was solved for nondeformable cables and then extended to find the solution for deformable cables. In [11], Irvine's sagging-cable model was linearized and used for a stability and stiffness analysis. The cable tensions were computed and used to solve an IK problem of spatial CDPRs.

Other approaches are also employed for kinematics and dynamics analyses, accounting for both the mass and elasticity of the cables. In [27], the port-Hamiltonian method was used to derive dynamic equations by calculating the MP's and cables' total kinetic and potential energies. In [12], a linear spring model with mass was used for the cables. Ordinary differential equations were derived using the lumped-mass method. The finite-difference method was used for the discretization of the equations. In [28], the same spring model was used for the cables. The Newton–Euler method was used to derive the dynamics equations considering the dynamics of actuators and pulleys.

Hefty elastic cable models are also used for stiffness analysis. In [75], the static stiffness was evaluated using the MP pose-error variation by considering a hefty elastic cable model for the cables. The dynamic stiffness was analyzed by identifying the robot's natural frequencies. In [49] and [76], the stiffness matrix of spatial CDPRs was calculated numerically. A homogenization of this stiffness matrix was introduced in [49] and can be used for design purposes.

Workspace

The CDPR workspace studies presented in the literature divide the overall workspace into three zones. A controllable or wrench-closure workspace (WCW) is related to every position of the MP in the configuration space, where the tensions in cables are greater than zero [77]. A wrench-feasible workspace (WFW) refers to the positions of the MP where a positive lower and upper bound are considered for the tension in cables, while the CDPR can resist any external wrenches in each set.

Workspace of Planar CDPRs

A 2–2 repetitive workspace IRPM with serial link support was presented in [78]. The robot was used for painting, and the repetitive workspace means that the BP can be shifted several times during the painting process. The effect of geometrical parameters, such as the anchor point's location for the serial manipulator on the workspace configuration, was analyzed.

For planar CRPMs, the WCW of a 4–3 CRPM with different MP angles was determined in [77], composed of conic sections. In [79], a variant of Bland's pivot rule was used to determine the WCW of planar and spatial CRPMs. A system of inequalities arising from static equilibrium was converted into a system of equations, which results in a more efficient workspace calculation compared to that obtained by numerical methods. In [80], the effect of prestressed cables on the WCW was reported. The prestress stable WCW was defined as a subset of the WCW, where an increase in the prestress level leads to an increase in the overall stiffness of the mechanism. In [35], a collision-free workspace of reconfigurable constrained robots in cluttered spaces was studied. The critical support lines of obstacles [Figure 5(a)], the topological constraints, and the convex hull-mapping method were used to define the collision-free workspace [Figure 5(b)]. Here, the critical support lines are determined by connecting the farthest points of two consecutive obstacles.

Workspace of Spatial CDPRs

Regarding the workspace of spatial IRPMs, the effects of different parameters, such as the size of the MP and BP and the MP rotation angle on the workspace geometry, were investigated in [81] and [82]. The results show that, when the degree of orientation of the MP is zero, the largest workspace is obtained. In [83], the boundaries of the WCW for spatial CDPRs with more than six cables were defined. For such robots, the WCW consists of cubic surfaces, like the WCW of the Gough–Stewart robot. In [84], a feasible dynamic workspace was determined analytically considering a prescribed set of accelerations for the MP. In [85], the improved workspace of a 4–6 IRPM was presented considering the inertia of MPs, external wrenches, and centrifugal and Coriolis matrices. However, it was shown that the improved workspace was around 32% smaller than the general workspace.

The workspace of a CDPR is always determined and characterized by the tension status of its driving cables. Therefore, the relative tension distribution among the cables is an appropriate measure to evaluate the quality of the

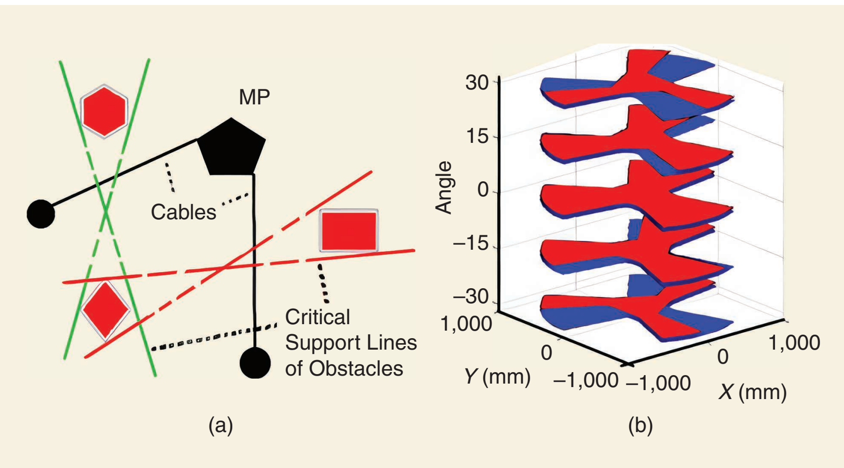

Figure 5. (a) Critical support lines of obstacles were used for defining the collision-free workspace, adapted from [35]. (b) The collision-free workspace of a three-cable CDPR with different orientations in a three-obstacle area [35].

workspace. In [86], the determination of an optimal tension factor value for generating an optimized workspace was studied. The tension factor was determined as the minimum tension over the maximum tension of the cables. When this factor approaches zero, the MP is located near the workspace boundary. By a similar analogy, if the factor approaches one, the MP is positioned far from the workspace boundary. In [38], a translational contour crafting RRPM with 12 cables was presented. The cable tensions were used to approximate the maximum structure size built using this manipulator, considering various loading conditions. In [87], the worst possible exerted wrench on the MP was considered the key wrench to define the controllable workspace of spatial CRPMs.

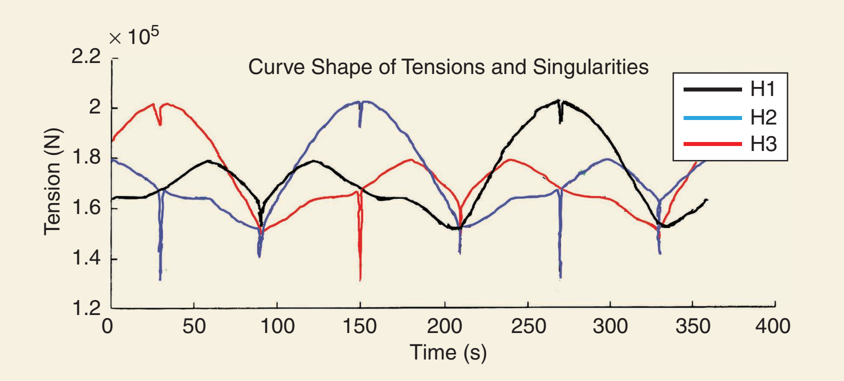

Figure 6. The curve shapes of tensions and resulting singularities of a CDPR with cables with mass. (Source: [88]; used with permission.)

For CDPRs with a large workspace, such as the FAST, the mass of cables was used for workspace analysis and studying the force singularities [88]. The plot of tension versus time (Figure 6) has six singular sections, where the cable tensions are uncertain. These six sections divide the shell workspace evenly into six segments. To tackle this problem, adding a tie-down cable for handling force singularities and improving the workspace was recommended.

In [89], an analytical solution method solved the static or quasi-static problem of the FAST. The calculation time of this method is lower than iterative methods, which makes it useful for real-time control. In [90], the kinetostatic solution of RRPMs for three different selection criteria consisting of 1) minimizing the tension in the cables, 2) maximizing the tension in the cables, and 3) minimizing the deviation between the cable tension and the mean tension is presented. Each criterion can be used for different applications with different requirements.

Workspace Optimization by Optimizing the Configuration

Two approaches are used in the literature for optimizing the workspace of CDPRs. The first approach analyzes the effect of different cable and motor configurations. The second approach considers integrating different elements, such as springs, into their structure.

The first approach was used to evaluate the WCW of two configurations of a 7–6 CRPM, "WIRO-6.1" and "WIRO-4.3," and a 9–6 RRPM, "WIRO-6.3," using numerical approaches [40]–[42]. The results showed that WIRO-6.3 has the largest workspace. The same approach was used in [39], and three different cable configurations of 7–6 CRPMs were compared. In [37], the maximum acceptable distance between the geometric center and the mass center of the MP was used as the performance index. The placement of motors and winches was optimized to have a more load-carrying capability with a larger workspace. In [36], Wire Center software was used to improve the rotational workspace of an 8–6 RRPM. Different cable configurations were tested to demonstrate that the cable configuration can increase the rotational workspace efficiently.

The second approach was used in [46], where an articulated gripper was integrated into the MP of a constrained robot. The gripper augments the boundaries of the workspace by grabbing an external structure, which allows the MP to reach outside its standard configuration space. In [45], springs were integrated into the structure of planar and spatial CRPMs (Figure 7). Their effect on the MP wrench was investigated by varying their number

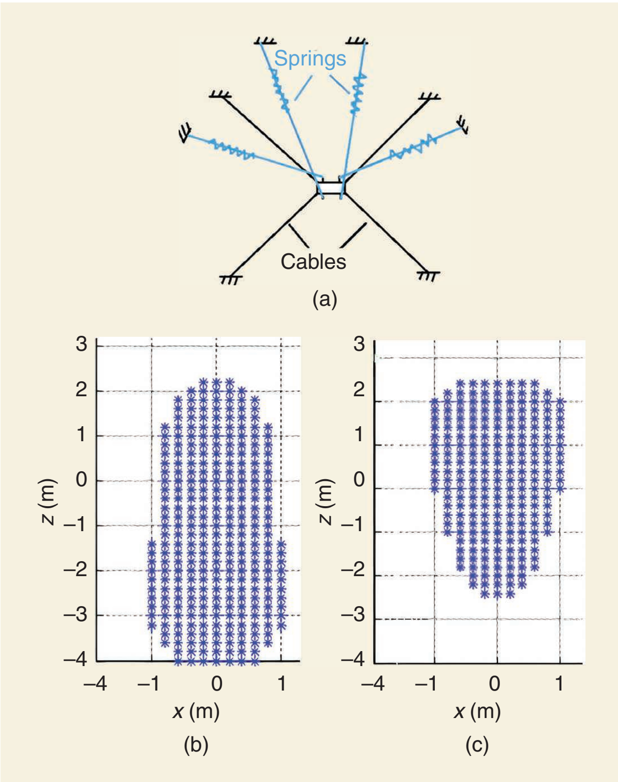

Figure 7. Integrating springs to CDPRs for having the desired workspace, b) workspace of the CDPR by adding springs, c) workspace without adding the springs. (Source: [45]; used with permission.)

and location. To maximize the WFW, the desirable spring parameters were calculated using a quadratic programming-based optimization scheme with lower and upper bounds on the cable tensions. In [44], a differential mechanism [Figure 8(a)] was used for pulling two cables using just one actuator. The workspace of a CRPM with and without this mechanism was analyzed using convex theory and linear algebra. In [43], a cable-loop structure [Figure 8(b)] was integrated into a planar CDPR to provide an unlimited and singularity-free orientation workspace. However, the cable loop also results in occasional rotational motions of the MP, so-called *parasitic inclinations*, which were modeled and assessed in this work.

For this robot, rotating arms were used at the top corners of the signpost for optimal force generation over the entire plane of the signpost.

Bar linkages and springs were used for the static balancing of a planar CDPR in [91]. This mechanism decreases the forces that must be applied to the MP across the workspace. It also helped to have a minimum desirable tension in the cables to conserve the workspace geometry.

Trajectory Planning

Trajectory planning of CDPRs is more challenging than for traditional parallel robots as the lengths and tensions of cables must remain within acceptable bounds to avoid cable sagging during operation [47], [48]. For CRPMs and RRPMs, all of the DoFs of the MP can be controlled, which makes the trajectory planning problem easier. For IRPMs, the WCW does not exist, which makes the trajectory planning complicated.

Trajectory Planning of Planar CDPRs

In terms of trajectory planning of IRPMs, a two-link serial robot was attached to the MP of a 2–2 IRPM to limit its out-of-plane motion in [92]. A numerical method was used to compute the minimum-time trajectory satisfying the velocity and acceleration constraints for a given path. Another 2–2 IRPM was introduced in [93] for removing graffiti from highway signs. For this robot, rotating arms were used at the top corners of the signpost for optimal force generation over the entire plane of the signpost. The workspace was divided into 20 sections wide by 20 sections high, and image processing was applied to isolate graffiti from nongraffiti in these sections. Then, the robot path was generated by connecting the coordinates of each section.

Regarding CRPMs and RRPMs, in [94], a reconfigurable 4–3 CRPM was designed for lower limb rehabilitation. The cable attachment points on the BP can move to balance the external wrenches during the limb motion. The area of the wrench-closure zone was increased for this mechanism using different actuation configurations.

Different methods are used for the minimum-time trajectory planning of CRPMs and RRPMs. In [50], the effects of the configuration of cables, the corresponding switching points, and the number of cables were optimized for the minimum-time trajectory planning of a 4–3 CRPM. In [59], a minimum-time trajectory-planning approach of redundant and nonredundant cable robots was presented. This approach reduced the differential equations of the robot dynamics to a system of second-order differential equations in terms of path parameters using the specified desired path.

Trajectory Planning of Spatial CDPRs

Most of the literature about the trajectory planning of spatial CDPRs is related to IRPMs. Point-to-point trajectory planning is one of the most frequent methods for spatial CDPRs, where different approaches are employed to ensure acceleration continuity and zero velocity at target points. In [95], a hypocycloid curve [Figure 9(a)] was used to connect the consecutive target points with zero instantaneous velocity to obtain the desired trajectory. Target points can be outside the static workspace of the mechanism, which guarantees a wider zone of achievable workspace. In [96], generic trajectory expressions of a 3–3 CDPR were derived using trigonometric functions. The feasible target points were defined, and viable areas between two consecutive points were selected for indirect trajectories. In [97], an $S-\ddot{S}$ plane was used to devise dynamically feasible point-to-point trajectories and periodic trajectories. In this approach, the unilateral cable tension constraints were explicitly converted to geometrical constraints in the $S-\ddot{S}$ plane.

The other approaches for the trajectory planning for CDPRs include an IRPM carrying a camera presented in [98]. This approach used the feedback of the current positions and velocities of the camera and the object to calculate the goal position and velocity of

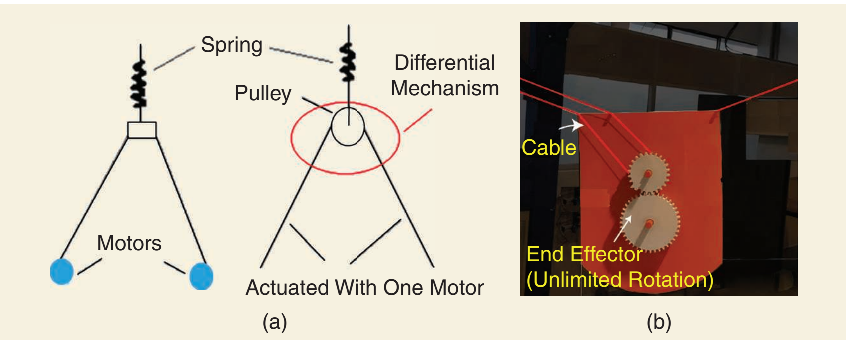

Figure 8. (a) A differential mechanism used for a CDPR instead of adding motors. (b) Increasing the rotational capability of CDPRs by cable loop. (Source: [43]; used with permission.)

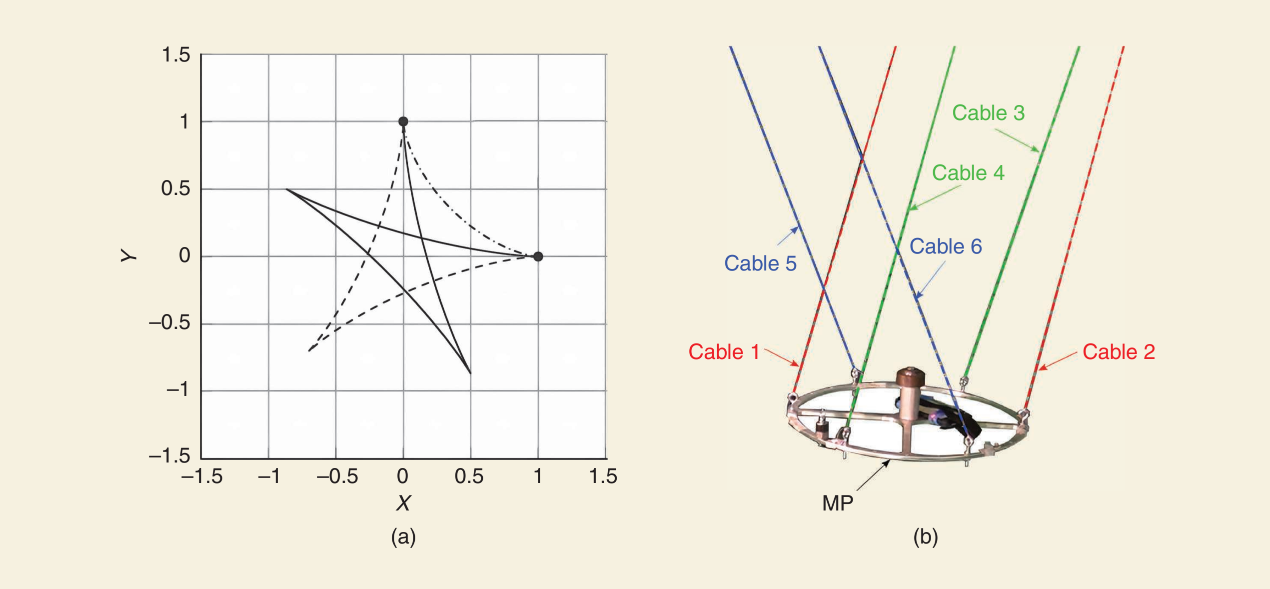

Figure 9. (a) Hypocycloid curves were used for trajectory planning with zero velocity at the target points [95]. (b) A 6–3 spatial RRPM equivalent to a 3–3 purely translational IRPM using a parallelogram. (Source: [99]; used with permission.)

the camera. In [99] and [100], a parallelogram configuration of cables was used to change the feasible dynamic motions of a 6–6 IRPM [Figure 9(b)]. Each parallelogram consists of two parallel cables sharing the same length. The robot can move like a 3–3 purely translational CDPR, while the MP orientation remains approximately the same.

Since fewer cables are used in IRPMs than CRPM or RRPM, the payload can have additional DoF and exhibit swaying motions or oscillations. A trajectory planner was implemented for a 4-6 IRPM to eliminate unwanted oscillations using a zero-vibration input-shaping scheme [101]. Motion in 3D space was mirrored to two vertical planes perpendicular to each other, and afterward, the natural frequency was calculated for planar IRPMs with two cables.

In terms of considering the mass and elasticity of the cables, a trajectory-planning approach was presented in [102] for a 6-6 IRPM considering a virtual equivalent spring model for the cables. The trajectory-planning technique permitted the MP to move beyond its static workspace in a controlled, predictable manner.

Regarding the trajectory planning of CRPMs and RRPMs, a robot was designed in [103] for simulating underwater forces, such as the buoyancy for a walking humanoid robot. The simulator robot followed the desired trajectories, ensuring a smooth path while avoiding any perturbation in the cables. In [104], the trajectory planning of a 4–3 CRPM for sensing and mapping of an aquatic environment was presented. Trajectory planning for minimum energy consumption when the robot is maneuvering periodic trajectories was determined. This was achieved by minimizing the second norm of the cable tension vector. A rapid calibration method was developed to reduce the deployment time using a laser rangefinder and plumb lines suspended from each cable origin. In this case, the horizontal distance between the plumb lines can be measured quickly and precisely.

In a cluttered environment, the cables can wrap around obstacles or tangle with each other [33]. Therefore, optimized collision-free path planning is studied in the literature to tackle this problem. In [33], a homotropy-signature augmented graph [Figure 10(a)] was used for path planning of an IRPM in an area with polygonal obstacles. Two different trajectories connecting the same start and end points are homotopic if one can continuously deform into the other without intersecting any obstacle.

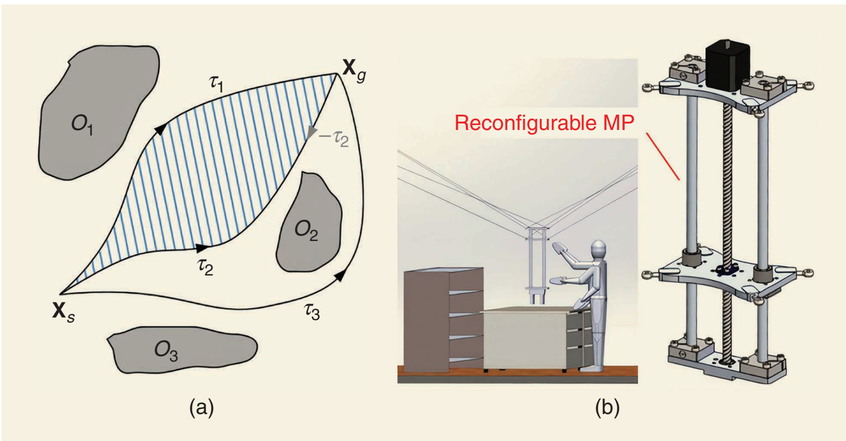

Figure 10. (a) τ_1 and τ_2 are homotopic, but τ_3 is not homotopic to τ_1 and τ_2 [33]. (b) A CDPR with a reconfigurable MP for collision-free path planning. (Source: [34]; used with permission.)

This approach helps to find the shortest path between the start and end points.

In [31], a piecewise linear interpolation method was introduced. In this approach, any target points above cable exit points can be connected in sequence via some intermediate points in the static workspace. Accordingly, the intermediate points can be accurately selected to avoid collisions between cables and obstacles. In [32], the path planning of a 6–6 IRPM was studied using the higher-dimensional continuation method of Henderson [105]. The approach provides a systematic way of transitioning through two configurations while ensuring cable tensions are inside their allowable bounds. The method is flexible enough to accommodate the collision constraints of the robot.

Changing the cable configuration at the MP or BP level is another approach to tackle cable and obstacle collisions. In [34], a reconfigurable MP [Figure 10(b)] was designed for pick and place in cluttered areas. The configuration of the MP can be changed to avoid collisions with obstacles while reducing the duration of motion.

In [30], the cable connection points on the BP can be positioned at a large but discrete set of possible locations ensuring minimal cable collisions. A feasibility map was generated to determine the minimum sets of configurations for following a prescribed path.

Control

Using cables makes the control of CDPRs more challenging than that for traditional rigid-link parallel robots. In this case, control laws should be designed to keep all tensions positive while attaining the desired control performance [106]. In addition, it is difficult to control the position and orientation of the MP precisely because of the low stiffness of such mechanisms. Therefore, some widely used control methods must be modified to meet the special properties of cables [48]. Both kinematic and dynamic controllers are implemented on CDPRs. Kinematic control techniques are based on an IK transformation [107], which feeds the reference values to the cables corresponding to the assigned MP trajectory. Dynamic controllers consider the nonlinear dynamics of the robot.

Control of CDPRs Assuming Massless Inelastic Cables

In terms of kinematic controllers, in [108], a proportional-derivative (PD) controller was used for a spatial object-tracking IRPM. The feedback from the gyro sensor, inertial measurement unit (IMU), and encoders were used for calculating position errors. In [109], a proportional-integral-derivative (PID) force servo system improved the loading accuracy and speed of a reconfigurable CDPR used for limb rehabilitation. The employed force servo system had a good tracking ability in the standard rehabilitation frequency band, meeting the requirements for rehabilitation. In [110], a two-part controller was designed for a 3–2 planar CRPM used for arm rehabilitation. The low-level controller was used for tension distribution through three cables, and the high-level controller was used for calculating assistive forces. The assistive force generated a virtual guidance field around a nominal path using impedance control to improve the movement accuracy and execution time.

In terms of dynamic controllers, feedback linearization (FL) control was used in [106] and [111] for CRPMs, ensuring positive tension in cables using linear and quadratic programming. The control input was chosen as $DV + G$, where $V = \ddot{e} - K_P e - K_D \dot{e}$, e is the error in position, and D and G are inertia and gravity matrices, respectively. In [112], FL control was augmented by adding a reference governor. This reference governor operates under the receding horizon strategy by generating admissible reference signals. This approach offered an efficient way to predict the system's future states using the error dynamics. In [113], the controller shortened the phase trajectory to dampen the oscillation of the nonlinear system. An oscillation number was defined as an index to evaluate the oscillatory nature of the nonlinear system, and the FL was used to minimize it.

Mechanical systems may interact with a disturbed environment [114]. Besides, there would be uncertainties in different mechanical parameters of the CDPRs, such as the mass and moment of inertia of the MP and the diameter of cable pulleys. Therefore, using adaptive and robust controllers can help achieve more accurate trajectory tracking. A robust PID controller was presented in [115] for a spatial CRPM to handle structured and unstructured uncertainties in the robot parameters, such as the mass and inertia of the MP. The vector of internal tension, which was obtained based on the null space of the robot's transposed Jacobian matrix, was used to ensure positive tension in the cables. To derive the control action $\bar{\tau}$, the pseudoinverse of the inaccurate Jacobian matrix $\hat{J}$ was used:

$$\bar{\tau} = \hat{J}(\hat{J}^T\hat{J})^{-1}\left(K_P e + K_D \dot{e} + K_I \int_0^t e(s)ds\right), \tag{4}$$

where e is the error in the position of the MP, and K_P, K_D, and K_I are positive definite diagonal gain matrices. In [116], three control algorithms—pole placement, sliding mode, and adaptive sliding mode—were implemented on a planar CRPM using feedback from a vision-based system. The adaptive sliding-mode controller had the best efficiency to handle uncertainties tackling the chattering phenomena. $S_k = K - K_{\text{reference}}$ was used as the sliding surfaces, where the elements in K and $K_{\text{reference}}$ corresponded to the x, y, and θ DoF of the MP.

Zarebidoki et al. [117] implemented an adaptive control algorithm and FL control on a 6–6 IRPM. The results were compared to demonstrate the efficiency of the adaptive controller to compensate for the uncertainties in the mass and moment of inertia of the MP and sinusoidal disturbances. In [118], a robust sliding-mode controller was implemented to a spatial IRPM carried by a helicopter. The helicopter produced gross motion, while the robot performed both translational and rotational movements. This method properly estimates the bound of the helicopter's motion, allowing the cable robot to be stabilized even when the helicopter's motion is unknown. In [119], an adaptive controller was implemented to eliminate cable interference in a spatial CRPM during translational motion. Repulsive forces were generated when cables were near to collision. The minimum distance between the two cables was calculated using the Karush–Kuhn–Tucker conditions method.

In [120], 2½D visual servo control was implemented on an 8–6 suspended RRPM. The vision algorithm provided feedback for the trajectory tracker to increase the robustness of the system. In [121], a nonlinear continuous-time generalized predictive control was used for a 4–2 RRPM. The controller design was based on the finite-horizon continuous-time minimization of a quadratic cost function. The cost function was chosen as the error between the desired trajectory and the predicted positions considering constraints on cable tensions. In [122], robust control of an 8–6 suspended RRPM balancing between PD and sliding-mode controllers was presented. The controller provides good accuracy and repeatability considering uncertainties in the MP's mass.

Neural network controllers, like one using an adaptive multilayer neural network, were presented in [123] for a planar IRPM to compensate for the perturbed conditions. A term was added to the central controller considering the dynamics of actuators and gearboxes to provide a priori bounded tension command for the cables. In [124], a neural network controller with an adjustable tracking error was used for a 4–3 planar rehabilitation robot. The controller aims to follow the desired trajectory by allowing an adjustable tracking error, enabling the human subject to freely move the limb inside this error area with an adjustable assistance level. The algorithm helps obtain a better rehabilitation efficiency using a compensating dynamic model implemented through an adaptive neural network.

In terms of fuzzy controllers, an adaptive control law was presented in [125] for a 3–6 upper limb rehabilitation IRPM. A fuzzy tuner was employed to adjust control parameters based on position errors in the presence of external uncertainties in the environment and time-varying dynamic properties of the human arm for the robot-aided rehabilitation.

In terms of RRPMs, along with an appropriate control scheme, a real-time embeddable algorithm for cable tension distribution is required. Therefore, different redundancy resolution approaches are used that also assist in ensuring positive tension in the cables. In [126], a noniterative real-time-compatible tension distribution algorithm within a dual-space feedforward scheme was implemented on an 8–6 suspended RRPM. In [127], an analytic–iterative scheme was used for redundancy resolution of a 4–2 RRPM. This scheme utilizes a convex optimization problem with inequality constraints of the manipulator structure and cable dynamics. The Karush–Kuhn–Tucker theorem is used to analyze the optimization problem, and a tractable and iterative search algorithm is proposed to implement the redundancy resolution. In [28], [128], and [129], the tension distributions of an 8-6 RRPM were studied by converting the problem into an optimization problem using p-norms of the cable tension as a cost function. In this approach, the tension distributions are continuous along trajectories and differentiable at most of the points. In [130], a new flexible cost function with the ability of intuitive tuning was used for the optimal tension distribution of different configurations of CDPRs. The cost function is chosen as a combination of fixed logarithmic barrier and p-norm functions. This method avoids undesired discontinuous accelerations of actuators and guarantees continuous differentiability of the actuator forces. In [131], a passive plant was established by considering cable pretension, which results in a strictly positive controller for planar RRPMs. The controller uses actuator saturation prevention techniques and the solution to a linear programming problem to ensure strictly positive tension in the cables. In [132], a model predictive-control strategy was used for RRPMs, explicitly addressing the cable tension limits. It means that the cable tension distribution can be performed as an integral part of the main model-based control architecture.

In terms of RRPMs, along with an appropriate control scheme, a real-time embeddable algorithm for cable tension distribution is required.

In [133], a new methodology for positive tension distribution in CDPRs without having any redundancy resolution approach is presented. The controller incorporates a positive saturation-type function to map the control effort into a positive range. In this case, a nonlinear disturbance observer compensates for the saturation effects. The stability of the proposed control scheme is verified through Lyapunov's second method.

Controllers Considering the Mass of Cables

The controllers reviewed in this section consider the mass and sagging of cables during the robot dynamics and aim to compensate for their effect for achieving exact positioning. A hybrid position/force PID controller was presented in [134] to tackle the pseudodrag problem of flexible cables in the FAST. The controller receives feedback from both the cable force error and position error. The tracking error achieved using this controller is about 2 mm, which assures the accuracy requirement for the FAST. In [135], a mobile wheeled CDPR was introduced, where the Gibbs–Appell method was used to derive the dynamics equation considering the mass of cables. This equation was used in the feedback law for FL to eliminate nonlinearities. The fuzzy method has also been used to control CDPRs with hefty cables and tune the controller gains. A fuzzy model reference learning controller was presented in [136] for a large-workspace robot, consisting of a direct fuzzy controller, a reference fuzzy inverse model, and a fuzzy learning part. The direct fuzzy controller was adjusted so that the closed-loop system acted like a prespecified reference model using the fuzzy learning mechanism.

In [137], an inverse dynamics analysis of the FAST was derived using the Lagrangian method. Random wind forces acting on the cabin (MP) were simulated, and a PD fuzzy controller was implemented to handle the vibrations induced by the wind. In [138], passivity-based control of a planar 2-1 CRPM using a modified input torque and output tip rate for establishing a passive input–output mapping was presented. A lumped-mass method was used to model the dynamics considering the changing stiffness and mass of the cable wrapped around a winch.

Controllers Considering the Elasticity of Cables

Different approaches are employed to control the effect of elasticity and vibration of CDPRs. One approach is to separate the fast and slow motion of the system. In [71], dynamic equations of a spatial IRPM were rewritten to the standard form of the singular perturbation approach. A corrective term was added to the rigid part of the controller to guarantee the asymptotic stability of the fast dynamics. The Tikhonov theorem was used to separate slow and fast variables for stability analysis. In [139], a composite robust adaptive method was presented for a 4–3 planar CRPM. A fast control term, $K_v(\dot{L}_1 - \dot{L}_2)$, was added to compensate for the longitudinal vibrations, where L_1 and L_2 are the vectors of the tensioned and free cable lengths, respectively, and K_v is a diagonal matrix. In [140], the MP's undesired vibration was separated from its desired equation of motion by neglecting the second- and higher-order terms of the motion errors to form a linear parametric variable dynamic system. A robust vibration compensator was designed using the H_∞ method to control the system.

In [23] and [141], PD, PID, and fuzzy PID controllers were used for a 7–6 spatial CRPM and a 4–3 planar CRPM. The fuzzy method was used to tune the gains of the PID controller, and an online dynamic minimum torque estimation was used to ensure positive tensions in the cables. System responses showed that the fuzzy PID controller is more robust than the PID controller when encountering disturbances from the elastic cables. IMUs and encoders were used to detect the fast and slow dynamic movements of the MP in [73]. Their feedback was used in the FL controller to estimate the precise position and orientation of the MP, and a Kalman filter was used to smooth the noises in the process.

In [72], the MP vibration was considered as a process noise. To achieve a tradeoff between the control input and the tracking error, the FL gains were obtained using the linear quadratic Gaussian method. A Lyapunov analysis demonstrated that a system with damping less than a specified minimum value could be stable with this approach. In [142], a mechanical reaction-based stabilizer was used for nonmodel-based vibration control of CDPRs. The stabilizer was composed of three actuators attached to a pendulum in a perpendicular arrangement mounted on the MP. The stabilizer needed only the actuators' directly measurable position and velocity to form its closed-loop control feedback signals. In [143], a linear decoupled model of an 8–6 suspended RRPM with elastic cables was derived using modal analysis. The model is projected in the modal space yielding six decoupled second-order transfer functions for six DoFs of the robot, which can be easily controlled with standard single-input, single-output techniques.

Conclusion and Outlook

In this review, different design configurations and applications of planar and spatial CDPRs have been presented. Along with reviewing new and emerging research aspects of CDPRs with massless inelastic cables, the effects of considering the mass and elasticity of cables on the kinematics, dynamics, and control were emphasized. Achieving configuration optimization by changing motor and cable placements or adding additional elements for having a larger workspace and collision-free trajectory planning were addressed. Moreover, robust and adaptive controllers for compensating uncertainties in the robot's parameters and disturbances were reported.

This review reveals some outstanding research aspects concerning the CDPRs, listed as follows.

1) In terms of considering the mass and elasticity of the cables, most of the literature considers linear behavior for the cables. The kinematics and dynamics considering the nonlinear elastic behavior of the thin cables still require investigation. Moreover, a framework for carrying out the comprehensive formulation for the kinematics and dynamics considering mass, nonlinear elasticity, and environmental effects, such as temperature and wind, still needs to be developed. Furthermore, only a few research works [69], [88], [102] have reported the effect of mass and elasticity of the cables on the workspace and trajectory planning.
2) While several investigations of CDPRs have been reported, the combination of traditional serial and parallel robots with CDPRs for constructing hybrid manipulators is still in its infancy. CDPRs can be integrated into traditional manipulators to cover some DoF of the system. However, kinematics, dynamics, workspace, trajectory planning, and control will require further investigation in such configurations.
3) The application of CDPRs for underwater applications or fluid environments has been little studied in the literature. However, a large workspace and lightweight structure can enable a CDPR to be suitable for such applications. This type of implementation requires considering the effect of fluid forces such as buoyancy and drag force on the MP and cables during dynamics analysis and control implementation. Efficient control algorithms need to be developed for such CDPR applications to handle the nonlinear dynamics arising from fluid forces.
4) CDPRs have several advantages over other robotic solutions in terms of easier modularity, scalability, and reconfigurability, which can be further enhanced by

optimal workspace generation and trajectory planning. Energy-efficient optimal trajectory planning for modular and reconfigurable CDPRs needs to be studied further to benefit applications having periodic and long-term use.

References

[1] S. Kawamura, H. Kino, and C. Won, "High-speed manipulation by using parallel wire-driven robots," *Robotica*, vol. 18, no. 1, pp. 13–21, Jan. 1, 2000, doi: 10.1017/S0263574799002477.

[2] A. Pott, *Cable-Driven Parallel Robots*, vol. 32. Cham, Switzerland: Springer-Verlag, 2018.

[3] S. E. Landsberger, *Design and Construction of a Cable-Controlled, Parallel Link Manipulator*. Massachusetts Inst. Technol., 1984.

[4] M. Tanaka, Y. Seguchi, and S. Shimada, "Kineto-statics of skycam-type wire transport system," in *Proc. USA—Japan Symp. Flexible Automat., Crossing Bridges: Adv. Flexible Automat. Robot.*, 1988, pp. 689–694.

[5] J. Albus, R. Bostelman, and N. Dagalakis, "The NIST robocrane," *J. Robot Syst.*, vol. 10, no. 5, pp. 709–724, Jul. 1993, doi: 10.1002/rob.4620100509.

[6] R. Kurtz and V. Hayward, "Dexterity measure for tendon actuated parallel mechanisms," in *Proc. 5th Int. Conf. Adv. Robot. 'Robots in Unstructured Environments'*, Italy, 1991, pp. 1141–1146, doi: 10.1109/ICAR.1991.240402.

[7] A. Ming and T. Higuchi, "Study on multiple degree-of-freedom positioning mechanism using wires," *Int. J. Japan Soc. Precision Eng.*, vol. 28, no. 2, pp. 131–138, 1994.

[8] M. J. Otis *et al.*, "Determination and management of cable interferences between two 6-DOF foot platforms in a cable-driven locomotion interface," *IEEE Trans. Syst., Man, Cybern.—Part A: Syst. Humans*, vol. 39, no. 3, pp. 528–544, May. 2009, doi: 10.1109/TSMCA.2009.2013188.

[9] Q. J. Duan, J. L. Du, B. Y. Duan, and A. F. Tang, "Deployment/retrieval modeling of cable-driven parallel robot," *Math. Problems Eng.*, vol. 2010, pp. 1–10, 2010.

[10] M. Gouttefarde, D. Q. Nguyen, and C. Baradat, "Kinetostatic analysis of cable-driven parallel robots with consideration of sagging and pulleys," in *Proc. 14th Int. Symp. Adv. Robot Kinematics*, Ljubljana, Slovenia, 2014, pp. 213–221.

[11] D. Q. Nguyen, M. Gouttefarde, O. Company, and F. Pierrot, "On the simplifications of cable model in static analysis of large-dimension cable-driven parallel robots," in *Proc. IEEE/RSJ Int. Conf. Intell. Robots Syst.*, Tokyo, Japan, Nov. 2013, pp. 928–934, doi: 10.1109/IROS.2013.6696461.

[12] J. Du, H. Bao, C. Cui, and D. Yang, "Dynamic analysis of cable-driven parallel manipulators with time-varying cable lengths," *Finite Elements Anal. Des.*, vol. 48, no. 1, pp. 1392–1399, 2012, doi: 10.1016/j.finel.2011.08.012.

[13] A. Tang, Y. Li, H. Qu, and J. Xiao, "Dynamics modeling and simulating analysis of a wire driven parallel mechanism," *Procedia Eng.*, vol. 15, pp. 788–794, 2011, doi: 10.1016/j.proeng.2011.08.147.

[14] Y. B. Bedoustani, P. Bigras, H. D. Taghirad, and I. A. Bonev, "Lagrangian dynamics of cable-driven parallel manipulators: A variable mass formulation," *Trans. Canadian Soc. Mech. Eng.*, vol. 35, no. 4, pp. 529–542, Dec. 2011, doi: 10.1139/tcsme-2011-0032.

[15] Q. J. Duan and X. C. Duan, "Analysis of cable-actuated parallel robot with variable length and velocity cable," *Procedia Eng.*, vol. 15, pp. 2732–2737, 2011, doi: 10.1016/j.proeng.2011.08.514.

[16] M. Gouttefarde, J. Collard, N. Riehl, and C. Baradat, "Simplified static analysis of large-dimension parallel cable-driven robots," in *Proc. IEEE Int. Conf. Robot. Automat.*, Saint Paul, MN, USA, May 2012, pp. 2299–2305, doi: 10.1109/ICRA.2012.6225159.

[17] R. Yao and H. Li, "A modeling method of the cable driven parallel manipulator for FAST," in *Proc. Cable-Driven Parallel Robots*, 2013, pp. 1–11.

[18] K. Kozak, Q. Zhou, and J. Wang, "Static analysis of cable-driven manipulators with non-negligible cable mass," *IEEE Trans. Robot.*, vol. 22, no. 3, pp. 425–433, Jun. 2006, doi: 10.1109/TRO.2006.870659.

[19] Y. X. Su, B. Y. Duan, R. D. Nan, and B. Peng, "Development of a large parallel-cable manipulator for the feed-supporting system of a next-generation large radio telescope," *J. Robot Syst.*, vol. 18, no. 11, pp. 633–643, Nov. 2001, doi: 10.1002/rob.8102.

[20] J. W. Jeong, S. H. Kim, Y. K. Kwak, and C. C. Smith, "Development of a parallel wire mechanism for measuring position and orientation of a robot end-effector," *Mechatronics*, vol. 8, no. 8, pp. 845–861, 1998, doi: 10.1016/S0957-4158(98)00034-8.

[21] R. Nan and D. Li, "The five-hundred-meter aperture spherical radio telescope (FAST) project," *IOP Conf. Ser.: Materials Sci. Eng.*, vol. 44, p. 12022, Apr. 23, 2013, doi: 10.1088/1757-899X/44/1/012022.

[22] J. Merlet, "MARIONET, a family of modular wire-driven parallel robots," in *Proc. Adv. Robot Kinematics: Motion Man Machine*, 2010, pp. 53–61, doi: 10.1007/978-90-481-9262-5_6.

[23] S. Kawamura, W. Choe, S. Tanaka, and S. R. Pandian, "Development of an ultrahigh speed robot FALCON using wire drive system," in *Proc. IEEE Int. Conf. Robot. Automat.*, Aichi, Japan, 1995, vol. 1, pp. 215–220, doi: 10.1109/ROBOT.1995.525288.

[24] G. Billette and C. Gosselin, "Producing rigid contacts in cable-driven haptic interfaces using impact generating reels," in *Proc. IEEE Int. Conf. Robot. Automat.*, Japan, May 2009, pp. 307–312, doi: 10.1109/ROBOT.2009.5152302.

[25] J. Merlet, "A generic numerical continuation scheme for solving the direct kinematics of cable-driven parallel robot with deformable cables," in *Proc. IEEE/RSJ Int. Conf. Intell. Robots Syst. (IROS)*, Daejeon, Korea, Oct. 2016, pp. 4337–4343, doi: 10.1109/IROS.2016.7759638.

[26] M. M. Aref, P. Gholami, and H. D. Taghirad, "Dynamic and sensitivity analysis of KNTU CDRPM: A cable driven redundant parallel manipulator," in *Proc. IEEE/ASME Int. Conf. Mechatron. Embedded Syst. Appl.*, Xi'an, China, Oct. 2008, pp. 528–533, doi: 10.1109/MESA.2008.4735650.

[27] C. Schenk, B. Yüksel, C. Secchi, and H. H. Bülthoff, "Port Hamiltonian modeling of a cable driven robot," *IFAC PapersOnLine*, vol. 51, no. 3, pp. 161–168, 2018, doi: 10.1016/j.ifacol.2018.06.047.

[28] P. Miermeister and A. Pott, "Modelling and real-time dynamic simulation of the cable-driven parallel robot IPAnema," *New Trends Mechanism Sci.*, vol. 5, pp. 353–360, Jul. 2010, doi: 10.1007/978-90-481-9689-0_41.

[29] X. Diao and O. Ma, "Vibration analysis of cable-driven parallel manipulators," *Multibody Syst. Dyn.*, vol. 21, no. 4, pp. 347–360, May 2009, doi: 10.1007/s11044-008-9144-0.

[30] L. Gagliardini, S. Caro, M. Gouttefarde, and A. Girin, "Discrete reconfiguration planning for cable-driven parallel robots," *Mechanism Mach. Theory*, vol. 100, pp. 313–337, Jun. 2016, doi: 10.1016/j.mechmachtheory.2016.02.014.

[31] N. Zhang, W. Shang, and S. Cong, "Dynamic trajectory planning for a spatial 3-DoF cable-suspended parallel robot," *Mechanism Mach. Theory*, vol. 122, pp. 177–196, Apr. 2018, doi: 10.1016/j.mechmachtheory.2017.12.023.

[32] O. Bohigas, M. Manubens, and L. Ros, "Planning Wrench-feasible motions for cable-driven hexapods," *IEEE Trans. Robot.*, vol. 32, no. 2, pp. 442–451, Apr. 2016, doi: 10.1109/TRO.2016.2529640.

[33] X. Wang and S. Bhattacharya, "A topological approach to workspace and motion planning for a cable-controlled robot in cluttered environments," *IEEE Robot. Automat. Lett.*, vol. 3, no. 3, pp. 2600–2607, Jul. 2018, doi: 10.1109/LRA.2018.2817684.

[34] L. Barbazza, F. Oscari, S. Minto, and G. Rosati, "Trajectory planning of a suspended cable driven parallel robot with reconfigurable end effector," *Robot. Comput. Integrated Manuf.*, vol. 48, pp. 1–11, Dec. 2017, doi: 10.1016/j.rcim.2017.02.001.

[35] B. Wang, B Zi, S Qian, and D Zhang, "Collision free force closure workspace determination of reconfigurable planar cable driven parallel robot," in *Proc. Asia-Pacific Conf. Intell. Robot Syst. (ACIRS)*, Tokyo, Japan, Jul. 2016, pp. 26–30, doi: 10.1109/ACIRS.2016.7556182.

[36] J. Seon, S. Park, S. Y. Ko, and J. Park, "Cable configuration analysis to increase the rotational range of suspended 6-DOF cable driven parallel robots," in *Proc. 16th Int. Conf. Control, Automat. Syst. (ICCAS)*, Gyeongju, Korea, Oct. 2016, pp. 1047–1052, doi: 10.1109/ICCAS.2016.7832438.

[37] M. Gouttefarde, J. Collard, N. Riehl, and C. Baradat, "Geometry selection of a redundantly actuated cable-suspended parallel robot," *IEEE Trans. Robot.*, vol. 31, no. 2, pp. 501–510, Apr. 2015, doi: 10.1109/TRO.2015.2400253.

[38] P. Bosscher, R. L. Williams, L. S. Bryson, and D. Castro-Lacouture, "Cable-suspended robotic contour crafting system," *Automat. Construction*, vol. 17, no. 1, pp. 45–55, 2007, doi: 10.1016/j.autcon.2007.02.011.

[39] X. Tang, L. Tang, J. Wang, and D. Sun, "Configuration synthesis for fully restrained 7-cable-driven manipulators," *Int. J. Adv. Robot. Syst.*, vol. 9, no. 4, p. 142, Oct. 2012, doi: 10.5772/52147.

[40] C. Ferraresi and F. Pescarmona, *Cable Driven Devices for Telemanipulation*. Croatia: IntechOpen, 2010. [Online]. Available: https://www.openaire.eu/search/publication?articleId=intech______::c5e977d68d69ad1bdeca41bbff6e13f9

[41] C. Ferraresi, M. Paoloni, and F. Pescarmona, "A new methodology for the determination of the workspace of six-DOF redundant parallel structures actuated by nine wires," *Robotica*, vol. 25, no. 1, pp. 113–120, Jan. 1, 2007, doi: 10.1017/S0263574706003055.

[42] C. Ferraresi, M. Paoloni, S. Pastorelli, and F. Pescarmona, "A new 6-DOF parallel robotic structure actuated by wires: The WiRo-6.3," *J. Robot Syst.*, vol. 21, no. 11, pp. 581–595, Nov. 2004, doi: 10.1002/rob.20037.

[43] S. Lessanibahri, P. Cardou, and S. Caro, "Parasitic inclinations in cable-driven parallel robots using cable loops," *Procedia CIRP*, vol. 70, pp. 296–301, 2018, doi: 10.1016/j.procir.2018.02.013.

[44] E. Stump and V. Kumar, "Workspaces of cable-actuated parallel manipulators," *J. Mech. Des.*, vol. 128, no. 1, p. 159, Jan. 1, 2006, doi: 10.1115/1.2121741.

[45] Q. Duan, V. Vashista, and S. K. Agrawal, "Effect on wrench-feasible workspace of cable-driven parallel robots by adding springs," *Mechanism Mach. Theory*, vol. 86, pp. 201–210, Apr. 2015, doi: 10.1016/j.mechmachtheory.2014.12.009.

[46] A. Martin, S. Caro, and P. Cardou, "Design of a cable-driven parallel robot with grasping device," *Procedia CIRP*, vol. 70, pp. 290–295, 2018, doi: 10.1016/j.procir.2018.03.105.

[47] C. Gosselin, "Cable-driven parallel mechanisms: State of the art and perspectives," *Mech. Eng. Rev.*, vol. 1, no. 1, p. DSM0004, 2014, doi: 10.1299/mer.2014dsm0004.

[48] S. Qian, B. Zi, W. Shang, and Q. Xu, "A review on cable-driven parallel robots," *Chin. J. Mech. Eng.*, vol. 31, no. 1, pp. 1–11, Dec. 2018, doi: 10.1186/s10033-018-0267-9.

[49] D. Q. Nguyen and M. Gouttefarde, "Stiffness matrix of 6-DOF cable-driven parallel robots and its homogenization," in *Proc. 14th Int. Symp. Adv. Robot Kinematic*, Slovenia, 2014, pp. 181–191.

[50] H. R. Fahham and M. Farid, "Optimum design of planar redundant cable-suspended robots for minimum time trajectory tracking," *ICCAS 2010*, pp. 2156–2163, Oct 2010. Korea,

[51] H. Khakpour, L. Birglen, and S. Tahan, "Synthesis of differentially driven planar cable parallel manipulators," *IEEE Trans. Robot.*, vol. 30, no. 3, pp. 619–630, Jun. 2014, doi: 10.1109/TRO.2013.2295891.

[52] A. Ming and T. Higuchi, "Study on multiple degree of freedom positioning mechanisms using wires," *Int. J. Japan Soc.*, vol. 28, no. 3, pp. 235–242, 1994.

[53] R. Verhoeven, *Analysis of the Workspace of Tendon Based Stewart Platforms*. Essen: Univ. of Duisburg, 2004.

[54] S. Behzadipour and A. Khajepour, "Design of reduced DOF parallel cable-based robots," *Mechanism Mach. Theory*, vol. 39, no. 10, pp. 1051–1065, 2004, doi: 10.1016/j.mechmachtheory.2004.05.003.

[55] Z. Zhang, Z. Shao, L. Wang, and A. J. Shih, "Optimal design of a high-speed pick-and-place cable-driven parallel robot," in *Proc. Cable-Driven Parallel Robots*, 2017, pp. 350–352, doi: 10.1007/978-3-319-61431-1_29.

[56] S. Behzadipour, "Kinematics and dynamics of a self-stressed cartesian cable-driven mechanism," *J. Mech. Des.*, vol. 131, no. 6, pp. 1–10, May 19, 2009.

[57] H. Liu, C. Gosselin, and T. Laliberté, "Conceptual design and static analysis of novel planar spring-loaded cable-loop-driven parallel mechanisms," *J. Mechanisms Robot.*, vol. 4, no. 2, May 1, 2012.

[58] J. Merlet, "On the inverse kinematics of cable-driven parallel robots with up to 6 sagging cables," in *Proc. IEEE/RSJ Int. Conf. Intell. Robots Syst. (IROS)*, Sep. 2015, pp. 4356–4361, doi: 10.1109/IROS.2015.7353995.

[59] H. R. Fahham and M. Farid, "Minimum-time trajectory planning of spatial cable-suspended robots along a specified path considering both tension and velocity constraints," *Eng. Optimization*, vol. 42, no. 4, pp. 387–402, Apr. 1, 2010, doi: 10.1080/03052150903247728.

[60] A. B. Alp and S. K. Agrawal, "Cable suspended robots: Design, planning and control," in *Proc. IEEE Int. Conf. Robot. Automat. (Cat. No.02CH37292)*, Washington, DC, USA, 2002, pp. 4275–4280, doi: 10.1109/ROBOT.2002.1014428.

[61] A. Afshari and A. Meghdari, "New Jacobian matrix and equations of motion for a 6 d.o.f cable-driven robot," *Int. J. Adv. Robot. Syst.*, vol. 4, no. 1, p. 8, Mar 1. 2007, doi: 10.5772/5709.

[62] A. Ghasemi, M. Eghtesad, and M. Farid, "Neural network solution for forward kinematics problem of cable robots," *J. Intell. Robot. Syst.*, vol. 60, no. 2, pp. 201–215, Nov. 2010, doi: 10.1007/s10846-010-9421-z.

[63] J. Collard and P. Cardou, "Computing the lowest equilibrium pose of a cable-suspended rigid body," *Optimization Eng.*, vol. 14, no. 3, pp. 457–476, Sep. 2013, doi: 10.1007/s11081-012-9191-5.

[64] S. Qian, B. Zi, D. Zhang, and L. Zhang, “Kinematics and error analysis of cooperative cable parallel manipulators for multiple mobile cranes,” *Int. J. Mech. Materials Des.*, vol. 10, no. 4, pp. 395–409, Dec. 2014, doi: 10.1007/s10999-014-9250-5.

[65] J. Qimi and V. Kumar, “The inverse kinematics of cooperative transport with multiple aerial robots,” *IEEE Trans. Robot.*, vol. 29, no. 1, pp. 136–145, Feb. 2013, doi: 10.1109/TRO.2012.2218991.

[66] B. P. Cong, Y. Guilin, and H. Y. Song, “Dynamic analysis of cable-driven parallel mechanisms,” in *Proc. IEEE/ASME Int. Conf. Adv. Intell. Mechatronics*, CA, USA, 2005, pp. 612–617, doi: 10.1109/AIM.2005.1511050.

[67] A. Gonzalez-Rodriguez, A. G. Gonzalez-Rodriguez, F. J. Castillo-Garcia, E. Ottaviano, and P. Rea, “On the effects of the design of cable-driven robots on kinematics and dynamics models accuracy,” *Mechatronics*, vol. 43, pp. 18–27, May 2017, doi: 10.1016/j.mechatronics.2017.02.002.

[68] B. Zi, J. Cao, H. Zhu, and H. Sun, “Comparative study of cable parallel manipulators with and without hybrid-driven planar five-bar mechanism,” *Appl. Math. Model.*, vol. 38, no. 24, pp. 5994–6017, Dec. 15, 2014, doi: 10.1016/j.apm.2014.05.002.

[69] A. Berti, J. Merlet, and M. Carricato, “Solving the direct geometrico-static problem of underconstrained cable-driven parallel robots by interval analysis,” *Int. J. Robot. Res.*, vol. 35, no. 6, pp. 723–739, May 2016, doi: 10.1177/0278364915595277.

[70] J. Merlet, “Kinematics of the wire-driven parallel robot MARIONET using linear actuators,” in *Proc. IEEE Int. Conf. Robot. Automat.*, Pasadena, CA, USA, May 2008, pp. 3857–3862, doi: 10.1109/ROBOT.2008.4543803.

[71] M. A. Khosravi and H. D. Taghirad, “Dynamic modeling and control of parallel robots with elastic cables: Singular perturbation approach,” *IEEE Trans. Robot.*, vol. 30, no. 3, pp. 694–704, Jun. 2014, doi: 10.1109/TRO.2014.2298057.

[72] M. Korayem, M. Yousefzadeh, and B. Beyranvand, “Dynamics and control of a 6-dof cable-driven parallel robot with visco-elastic cables in presence of measurement noise,” *J. Intell. Robot. Syst.*, vol. 88, no. 1, pp. 73–95, Oct. 2017, doi: 10.1007/s10846-017-0546-1.

[73] M. H. Korayem, M. Yousefzadeh, and S. Kian, “Precise end-effector pose estimation in spatial cable-driven parallel robots with elastic cables using a data fusion method,” *Measurement*, vol. 130, pp. 177–190, Dec. 2018, doi: 10.1016/j.measurement.2018.08.009.

[74] H. M. Irvine, *Cable Structures.* Cambridge, MA, USA: MIT Press, 1981.

[75] H. Yuan, E. Courteille, and D. Deblaise, “Static and dynamic stiffness analyses of cable-driven parallel robots with non-negligible cable mass and elasticity,” *Mechanism Mach. Theory*, vol. 85, no. 85, pp. 64–81, Mar. 2015, doi: 10.1016/j.mechmachtheory.2014.10.010.

[76] M. Arsenault, “Workspace and stiffness analysis of a three-degree-of-freedom spatial cable-suspended parallel mechanism while considering cable mass,” *Mechanism Mach. Theory*, vol. 66, pp. 1–13, Aug. 2013, doi: 10.1016/j.mechmachtheory.2013.03.003.

[77] M. Gouttefarde and C. M. Gosselin, “On the properties and the determination of the wrench-closure workspace of planar parallel cable-driven mechanisms,” in *Proc. ASME Des. Eng. Tech. Conf.*, Utah, USA, 2004, p. 10.

[78] M. Seriani, S. Seriani, and P. Gallina, “Workspace optimization for a planar cable-suspended direct-driven robot,” *Robot. Comput. Integr. Manuf.*, vol. 34, pp. 1–7, Aug. 2015, doi: 10.1016/j.rcim.2015.01.004.

[79] A. Ghasemi, M. Eghtesad, and M. Farid, “Workspace analysis for planar and spatial redundant cable robots,” *J. Mechanisms Robot.*, vol. 1, no. 4, p. 44502, 2009, doi: 10.1115/1.3211026.

[80] M. Arsenault, “Optimization of the prestress stable wrench closure workspace of planar parallel three-degree-of-freedom cable-driven mechanisms with four cables,” in *Proc. IEEE Int. Conf. Robot. Automat.*, Alaska, May 2010, pp. 1182–1187.

[81] J. Pusey, A. Fattah, S. Agrawal, and E. Messina, “Design and workspace analysis of a 6–6 cable-suspended parallel robot,” *Mechanism Mach. Theory*, vol. 39, no. 7, pp. 761–778, 2004, doi: 10.1016/j.mechmachtheory.2004.02.010.

[82] J. Hamedi and H. Zohoor, “Kinematic modeling and workspace analysis of a spatial cable suspended robot as incompletely restrained positioning mechanism,” *Int. J. Mech. Mechatron. Eng.*, vol. 2, no. 2, pp. 179–188, 2008.

[83] M. Gouttefarde, J. Merlet, and D. Daney, “Determination of the wrench-closure workspace of 6-DOF parallel cable-driven mechanisms,” in *Proc. Adv. Robot Kinematics,* 2006, pp. 315–322.

[84] G. Barrette and C. M. Gosselin, “Determination of the dynamic workspace of cable-driven planar parallel mechanisms,” *J. Mech. Des. (1990)*, vol. 127, no. 2, pp. 242–248, Mar. 1, 2005, doi: 10.1115/1.1830045.

[85] L. Gagliardini, M. Gouttefarde, and S. Caro, “Determination of a dynamic feasible workspace for cable-driven parallel robots,” HAL Open Science, 2017, pp. 361–370. [Online]. Available: https://hal.archives-ouvertes.fr/hal-01758038

[86] G. Yang, C. B. Pham, and S. H. Yeo, “Workspace performance optimization of fully restrained cable-driven parallel manipulators,” in *Proc. IEEE/RSJ Int. Conf. Intell. Robots Syst.*, Beijing, China, Oct. 2006, pp. 85–90, doi: 10.1109/IROS.2006.281747.

[87] A. Z. Loloei and H. D. Taghirad, “Controllable workspace of cable-driven redundant parallel manipulators by fundamental wrench analysis,” *Trans. Canadian Soc. Mech. Eng.*, vol. 36, no. 3, pp. 297–314, Sep. 2012, doi: 10.1139/tcsme-2012-0021.

[88] Y. Y. Qiu, B. Y. Duan, Q. Wei, and J. L. Du, “Elimination of force singularity of the cable and cabin structure for the next generation large radio telescope,” *Mechatronics*, vol. 12, no. 7, pp. 905–918, 2002, doi: 10.1016/S0957-4158(01)00035-6.

[89] J. Yin, P. Jiang, and R. Yao, “An approximately analytical solution method for the cable-driven parallel robot in FAST,” *Res. Astronomy Astrophys.*, vol. 21, no. 2, p. 46, Mar. 1, 2021, doi: 10.1088/1674-4527/21/2/46.

[90] I. Chawla, P. M. Pathak, L. Notash, A. K. Samantaray, Q. Li, and U. K. Sharma, “Effect of selection criterion on the kineto-static solution of a redundant cable-driven parallel robot considering cable mass and elasticity,” *Mechanism Mach. Theory*, vol. 156, p. 104175, Feb. 2021, doi: 10.1016/j.mechmachtheory.2020.104175.

[91] S. Perreault, P. Cardou, and C. Gosselin, “Approximate static balancing of a planar parallel cable-driven mechanism based on four-bar linkages and springs,” *Mechanism Mach. Theory*, vol. 79, pp. 64–79, Sep. 2014, doi: 10.1016/j.mechmachtheory.2014.04.008.

[92] A. Trevisani, “Underconstrained planar cable-direct-driven robots: A trajectory planning method ensuring positive and bounded cable tensions,” *Mechatronics*, vol. 20, no. 1, pp. 113–127, 2010, doi: 10.1016/j.mechatronics.2009.09.011.

[93] S. P. Donohoe, S. A. Velinsky, and T. A. Lasky, “Mechatronic implementation of a force optimal underconstrained planar cable robot,” *IEEE/ASME Trans. Mechatron.*, vol. 21, no. 1, pp. 69–78, Feb. 2016, doi: 10.1109/TMECH.2015.2431192.

[94] G. Abbasnejad, J. Yoon, and H. Lee, "Optimum kinematic design of a planar cable-driven parallel robot with wrench-closure gait trajectory," *Mechanism Mach. Theory*, vol. 99, pp. 1–18, May 2016, doi: 10.1016/j.mechmachtheory.2015.12.009.

[95] P. Dion-Gauvin and C. Gosselin, "Dynamic point-to-point trajectory planning of a three-DOF cable-suspended mechanism using the hypocycloid curve," *IEEE/ASME Trans. Mechatron.*, vol. 23, no. 4, pp. 1964–1972, Aug. 2018, doi: 10.1109/TMECH.2018.2840051.

[96] X. Jiang and C. Gosselin, "Dynamic point-to-point trajectory planning of a three-DOF cable-suspended parallel robot," *IEEE Trans. Robot.*, vol. 32, no. 6, pp. 1550–1557, Dec. 2016, doi: 10.1109/TRO.2016.2597315.

[97] N. Zhang, W. Shang, and S. Cong, "Geometry-based trajectory planning of a 3-3 cable-suspended parallel robot," *IEEE Trans. Robot.*, vol. 33, no. 2, pp. 484–491, Apr. 2017, doi: 10.1109/TRO.2016.2631591.

[98] L. Kevac, M. Filipovic, and A. Rakic, "The trajectory generation algorithm for the cable-suspended parallel robot—The CPR Trajectory Solver," *Robot. Autonom. Syst.*, vol. 94, pp. 25–33, Aug. 2017, doi: 10.1016/j.robot.2017.04.018.

[99] G. Mottola, C. Gosselin, and M. Carricato, "Dynamically feasible motions of a class of purely-translational cable-suspended parallel robots," *Mechanism Mach. Theory*, vol. 132, pp. 193–206, Feb. 2019, doi: 10.1016/j.mechmachtheory.2018.10.017.

[100] D. Vu, E. Barnett, A. Zaccarin, and C. Gosselin, "On the design of a three-DOF cable-suspended parallel robot based on a parallelogram arrangement of the cables," in *Cable-Driven Parallel Robots*, C. Gosselin, P. Cardou, T. Bruckmann, and A. Pott, Eds. Cham, Switzerland: Springer International Publishing, 2018, pp. 319–330.

[101] S. Hwang, J. Bak, J. Yoon, J. Park, and J. Park, "Trajectory generation to suppress oscillations in under-constrained cable-driven parallel robots," *J. Mech. Sci. Technol.*, vol. 30, no. 12, pp. 5689–5697, Dec. 2016, doi: 10.1007/s12206-016-1139-9.

[102] X. Jiang, E. Barnett, and C. Gosselin, "Periodic trajectory planning beyond the static workspace for 6-DOF cable-suspended parallel robots," *IEEE Trans. Robot.*, vol. 34, no. 4, pp. 1128–1140, Aug. 2018, doi: 10.1109/TRO.2018.2819668.

[103] A. R. Barroso, R. Saltaren, G. Portilla, J. S. Cely, and M. Carpio, "Smooth path planner for dynamic simulators based on cable-driven parallel robots," in *Proc. Int. Conf. Smart Syst. Technol. (SST)*, Oct. 2018, pp. 145–150, doi: 10.1109/SST.2018.8564635.

[104] P. H. Borgstrom *et al.*, "Design and implementation of NIMS3D, a 3-D cabled robot for actuated sensing applications," *IEEE Trans. Robot.*, vol. 25, no. 2, pp. 325–339, Apr. 2009, doi: 10.1109/TRO.2009.2012339.

[105] M. Henderson, "Multiple parameter continuation: Computing implicitly defined k-manifolds," *Int. J. Bifurcation Chaos*, vol. 12, no. 3, pp. 451–476, Mar. 2002, doi: 10.1142/S0218127402004498.

[106] S.-R. Oh and S. K. Agrawal, "Cable suspended planar robots with redundant cables: Controllers with positive tensions," *IEEE Trans. Robot.*, vol. 21, no. 3, pp. 457–465, Jun. 2005, doi: 10.1109/TRO.2004.838029.

[107] G. Antonelli, S. Chiaverini, and G. Fusco, "Kinematic control of redundant manipulators with on-line end-effector path tracking capability under velocity and acceleration constraints," *IFAC Proc. Vol.*, vol. 33, no. 27, pp. 183–188, Sep. 2000, doi: 10.1016/S1474-6670(17)37926-0.

[108] A. Aflakian, A. Safaryazdi, M. Tale Masouleh, and A. Kalhor, "Experimental study on the kinematic control of a cable suspended parallel robot for object tracking purpose," *Mechatronics*, vol. 50, pp. 160–176, Apr. 2018, doi: 10.1016/j.mechatronics.2018.02.005.

[109] Y. Zou, N. Wang, X. Wang, H. Ma, and K. Liu, "Design and experimental research of movable cable-driven lower limb rehabilitation robot," *IEEE Access*, vol. 7, pp. 2315–2326, Dec. 2018, doi: 10.1109/ACCESS.2018.2887233.

[110] D. Zanotto, G. Rosati, S. Minto, and A. Rossi, "Sophia-3: A semi-adaptive cable-driven rehabilitation device with a tilting working plane," *IEEE Trans. Robot.*, vol. 30, no. 4, pp. 974–979, Aug. 2014, doi: 10.1109/TRO.2014.2301532.

[111] S. Oh and S. K. Agrawal, "The feasible workspace analysis of a set point control for a cable-suspended robot with input constraints and disturbances," *IEEE Trans. Control Syst. Technol.*, vol. 14, no. 4, pp. 735–742, Jul. 2006, doi: 10.1109/TCST.2006.872515.

[112] S. Oh and S. K. Agrawal, "A reference governor-based controller for a cable robot under input constraints," *IEEE Trans. Control Syst. Technol.*, vol. 13, no. 4, pp. 639–645, Jul. 2005, doi: 10.1109/TCST.2004.841668.

[113] M. Zarei, A. Aflakian, A. Kalhor, and M. T. Masouleh, "Oscillation damping of nonlinear control systems based on the phase trajectory length concept: An experimental case study on a cable-driven parallel robot," *Mechanism Mach. Theory*, vol. 126, pp. 377–396, Aug. 2018, doi: 10.1016/j.mechmachtheory.2018.04.007.

[114] H. Jia, W. Shang, F. Xie, B. Zhang, and S. Cong, "Second-order sliding-mode-based synchronization control of cable-driven parallel robots," *IEEE/ASME Trans. Mechatron.*, vol. 25, no. 1, pp. 383–394, Feb. 2020, doi: 10.1109/TMECH.2019.2960048.

[115] M. A. Khosravi and H. D. Taghirad, "Robust PID control of fully-constrained cable driven parallel robots," *Mechatronics*, vol. 24, no. 2, pp. 87–97, Mar. 2014, doi: 10.1016/j.mechatronics.2013.12.001.

[116] H. Bayani, M. T. Masouleh, and A. Kalhor, "An experimental study on the vision-based control and identification of planar cable-driven parallel robots," *Robot. Autonom. Syst.*, vol. 75, pp. 187–202, Jan. 2016, doi: 10.1016/j.robot.2015.10.002.

[117] M. Zarebidoki, A. Lotfavar, and H. R. Fahham, "Dynamic modeling and adaptive control of a cable-suspended robot," in *Proc. World Congr. Eng.,* 2011, pp. 2469–2473.

[118] S. Oh, J. Ryu, and S. K. Agrawal, "Dynamics and control of a helicopter carrying a payload using a cable-suspended robot," *J. Mech. Des.*, vol. 128, no. 5, pp. 1113, Sep. 1, 2006, doi: 10.1115/1.2218882.

[119] R. Meziane, P. Cardou, and M. J. Otis, "Cable interference control in physical interaction for cable-driven parallel mechanisms," *Mechanism Mach. Theory*, vol. 132, pp. 30–47, Feb. 2019, doi: 10.1016/j.mechmachtheory.2018.10.002.

[120] Z. Zake, F. Chaumette, N. Pedemonte, and S. Caro, "Robust 2½D visual servoing of a cable-driven parallel robot thanks to trajectory tracking," *IEEE Robot. Automat. Lett.*, vol. 5, no. 2, pp. 660–667, Apr. 2020, doi: 10.1109/LRA.2020.2965033.

[121] F. Inel, A. Medjbouri, and G. Carbone, "A nonlinear continuous-time generalized predictive control for a planar cable-driven parallel robot," *Actuators*, vol. 10, no. 5, p. 97, May 4, 2021, doi: 10.3390/act10050097.

[122] E. Picard, E. Tahoumi, F. Plestan, S. Caro, and F. Claveau, "A new control scheme of cable-driven parallel robot balancing between sliding mode and linear feedback," *IFAC PapersOnLine*, vol. 53, no. 2, pp. 9936–9943, 2020, doi: 10.1016/j.ifacol.2020.12.2708.

[123] H. Jabbari Asl and F. Janabi-Sharifi, “Adaptive neural network control of cable-driven parallel robots with input saturation,” *Eng. Appl. Artif. Intell.*, vol. 65, pp. 252–260, Oct. 2017, doi: 10.1016/j.engappai.2017.05.011.

[124] H. Asl and J. Yoon, “Stable assist-as-needed controller design for a planar cable-driven robotic system,” *Int. J. Control, Automat. Syst.*, vol. 15, no. 6, pp. 2871–2882, Dec. 2017, doi: 10.1007/s12555-016-0492-x.

[125] J. Yang, H. Su, Z. Li, D. Ao, and R. Song, “Adaptive control with a fuzzy tuner for cable-based rehabilitation robot,” *Int. J. Control, Automat. Syst.*, vol. 14, no. 3, pp. 865–875, Jun. 2016, doi: 10.1007/s12555-015-0049-4.

[126] J. Lamaury and M. Gouttefarde, “Control of a large redundantly actuated cable-suspended parallel robot,” in *Proc. 30th IEEE Int. Conf. Robot. Automat.*, May 2013, pp. 4644–4649, doi: 10.1109/ICRA.2013.6631240.

[127] H. D. Taghirad and Y. B. Bedoustani, “An analytic-iterative redundancy resolution scheme for cable-driven redundant parallel manipulators,” *IEEE Trans. Robot.*, vol. 27, no. 6, pp. 1137–1143, Dec. 2011, doi: 10.1109/TRO.2011.2163433.

[128] C. Gosselin and M. Grenier, “On the determination of the force distribution in overconstrained cable-driven parallel mechanisms,” *Meccanica (Milan)*, vol. 46, no. 1, pp. 3–15, Feb. 2011, doi: 10.1007/s11012-010-9369-x.

[129] A. Pott, T. Bruckmann, and L. Mikelsons, “Closed-form force distribution for parallel wire robots,” in *Computational Kinematics*, A. Kecskeméthy and A. Müller, Eds. Cham, Switzerland: Springer-Verlag, 2009, pp. 25–34. [Online]. Available: http://link.springer.com/10.1007/978-3-642-01947-0_4

[130] E. Ueland, T. Sauder, and R. Skjetne, “Optimal force allocation for overconstrained cable-driven parallel robots: continuously differentiable solutions with assessment of computational efficiency,” *IEEE Trans. Robot.*, vol. 37, no. 2, pp. 659–666, Apr. 2021, doi: 10.1109/TRO.2020.3020747.

[131] R. J. Caverly and J. R. Forbes, “Flexible cable-driven parallel manipulator control: maintaining positive cable tensions,” *IEEE Trans. Control Syst. Technol.*, vol. 26, no. 5, pp. 1874–1883, Sep. 2018, doi: 10.1109/TCST.2017.2728007.

[132] J. C. Santos, A. Chemori, and M. Gouttefarde, “Redundancy resolution integrated model predictive control of CDPRs: Concept, implementation and experiments,” in *Proc. IEEE Int. Conf. Robot. Automat. (ICRA)*, May 2020, pp. 3889–3895, doi: 10.1109/ICRA40945.2020.9197271.

[133] A. Ameri, A. Molaei, and M. A. Khosravi, “Nonlinear observer-based tension distribution for cable-driven parallel robots,” in *Proc. Int. Conf. Cable-Driven Parallel Robots.* Cham, Switzerland, Jun. 2021, pp. 105–116.

[134] X. Tang and Z. Shao, “Trajectory generation and tracking control of a multi-level hybrid support manipulator in FAST,” *Mechatronics*, vol. 23, no. 8, pp. 1113–1122, Dec. 2013, doi: 10.1016/j.mechatronics.2013.09.002.

[135] M. Korayem, M. Yousefzadeh, and S. Susany, “Dynamic modeling and feedback linearization control of wheeled mobile cable-driven parallel robot considering cable sag,” *Arab. J. Sci. Eng.*, vol. 42, no. 11, pp. 4779–4788, Nov. 2017, doi: 10.1007/s13369-017-2658-0.

[136] Y. X. Su, C. H. Zheng, and B. Y. Duan, “Fuzzy learning tracking of a parallel cable manipulator for the square kilometre array,” *Mechatronics*, vol. 15, no. 6, pp. 731–746, 2005, doi: 10.1016/j.mechatronics.2004.12.001.

[137] B. Zi, B. Y. Duan, J. L. Du, and H. Bao, “Dynamic modeling and active control of a cable-suspended parallel robot,” *Mechatronics*, vol. 18, no. 1, pp. 1–12, 2008, doi: 10.1016/j.mechatronics.2007.09.004.

[138] R. J. Caverly, J. R. Forbes, and D. Mohammadshahi, “Dynamic modeling and passivity-based control of a single degree of freedom cable-actuated system,” *IEEE Trans. Control Syst. Technol.*, vol. 23, no. 3, pp. 898–909, May 2015, doi: 10.1109/TCST.2014.2347807.

[139] R. Babaghasabha, M. Khosravi, and H. Taghirad, “Adaptive robust control of fully constrained cable robots: Singular perturbation approach,” *Nonlinear Dyn.*, vol. 85, no. 1, pp. 607–620, Jul. 2016, doi: 10.1007/s11071-016-2710-8.

[140] H. Jamshidifar, S. Khosravani, B. Fidan, and A. Khajepour, “Vibration decoupled modeling and robust control of redundant cable-driven parallel robots,” *IEEE/ASME Trans. Mechatron.*, vol. 23, no. 2, pp. 690–701, Apr. 2018, doi: 10.1109/TMECH.2018.2793578.

[141] F. Najafi and M. Bakhshizadeh, “Development a fuzzy PID controller for a parallel cable robot with flexible cables,” in *Proc. 4th Int. Conf. Robot. Mechatron. (ICROM)*, Oct. 2016, pp. 90–97, doi: 10.1109/ICRoM.2016.7886823.

[142] H. Jamshidifar, M. Rushton, and A. Khajepour, “A reaction-based stabilizer for nonmodel-based vibration control of cable-driven parallel robots,” *IEEE Trans. Robot.*, vol. 37, no. 2, pp. 667–674, Apr. 2021, doi: 10.1109/TRO.2020.3031269.

[143] L. Cuvillon, X. Weber, and J. Gangloff, “Modal control for active vibration damping of cable-driven parallel robots,” *J. Mechanisms Robot.*, vol. 12, no. 5, Oct. 1, 2020, doi: 10.1115/1.4046434.

[144] F. Ennaiem *et al.*, “Task-based design approach: Development of a planar cable-driven parallel robot for upper limb rehabilitation,” *Appl. Sci.*, vol. 11, no. 12, p. 5635, Jun. 2021, doi: 10.3390/app11125635.

[145] L. Zhang, L. Li, Y. Zou, K. Wang, X. Jiang, and H. Ju, “Force control strategy and bench press experimental research of a cable driven astronaut rehabilitative training robot,” *IEEE Access*, vol. 5, pp. 9981–9989, May 2017, doi: 10.1109/ACCESS.2017.2702188.

[146] T. Zhao, S. Qian, Q. Chen, and Z. Sun, “Design and analysis of a cable-driven parallel robot for waist rehabilitation,” in *Proc. IEEE Int. Conf. Mechatron., Robot. Automat. (ICMRA)*, May 2018, pp. 173–178, doi: 10.1109/ICMRA.2018.8490581.

[147] L. Dovat *et al.*, “HandCARE: A cable-actuated rehabilitation system to train hand function after stroke,” *IEEE Trans. Neural Syst. Rehabil. Eng.*, vol. 16, no. 6, pp. 582–591, Dec. 2008, doi: 10.1109/TNSRE.2008.2010347.

[148] R. Beer, C. Naujokas, B. Bachrach, and D. Mayhew, “Development and evaluation of a gravity compensated training environment for robotic rehabilitation of post-stroke reaching,” in *Proc. 2nd Biennial IEEE/RAS-EMBS Int. Conf. Biomed. Robot. Biomechatron.*, USA, 2008, pp. 205–210.

[149] A. Alamdari and V. Krovi, “A cable-driven robotic rehabilitation system for lower-extremity motor therapy,” in *Proc. ASME 2015 Int. Design Eng. Techn. Conf. Comput. Inf. Eng. Conf.*, USA, Aug. 2, 2015, pp. 1–10.

[150] S. Bennour, M. Harshe, L. Romdhane, and J. Merlet, “A new experimental set-up based on a parallel cable robot for analysis and control of human motion,” *Comput. Methods Biomech. Biomed. Eng.*, vol. 14, pp. 83–85, Aug. 1, 2011, doi: 10.1080/10255842.2011.592372.

[151] G. Rosati, P. Gallina, and S. Masiero, “Design, implementation and clinical tests of a wire-based robot for neurorehabilitation,” *IEEE Trans. Neural Syst. Rehabil. Eng.*, vol. 15, no. 4, pp. 560–569, Dec. 2007, doi: 10.1109/TNSRE.2007.908560.

[152] H. Vallery *et al.*, “Multidirectional transparent support for overground gait training,” in *Proc. IEEE 13th Int. Conf. Rehab. Robot. (ICORR)*, United States, Jun. 2013, pp. 1–7.

[153] Y. Wang, K. Wang, and Z. Zhang, "Design, comprehensive evaluation, and experimental study of a cable-driven parallel robot for lower limb rehabilitation," *J. Brazilian Soc. Mech. Sci. Eng.*, vol. 42, no. 7, p. 371, Jul. 2020.

[154] F. Ennaiem *et al.*, "Sensitivity based selection of an optimal cable-driven parallel robot design for rehabilitation purposes," *Robotics (Basel)*, vol. 10, no. 1, p. 7, Jan. 1, 2021, doi: 10.3390/robotics10010007.

[155] C. M. Gosselin and S. Perreault, "Cable-driven parallel mechanisms: Application to a locomotion interface." *ASME. J. Mech. Des*., pp. 1–8, vol. 130, no. 10, Oct. 2008, Art. no. 102301. [Online]. Available: https://doi.org/10.1115/1.2965607

[156] J. Izard *et al.*, "Large-scale 3D printing with cable-driven parallel robots," *Construction Robot.*, vol. 1, nos. 1–4, pp. 69–76, Dec. 2017, doi: 10.1007/s41693-017-0008-0.

[157] E. Barnett and C. Gosselin, "Large-scale 3D printing with a cable-suspended robot," *Additive Manuf.*, vol. 7, pp. 27–44, Jul. 2015, doi: 10.1016/j.addma.2015.05.001.

[158] J. Jung, "Workspace and stiffness analysis of 3D printing cable-driven parallel robot with a retractable beam-type end-effector," *Robotics (Basel)*, vol. 9, no. 3, p. 65, Aug. 24, 2020, doi: 10.3390/robotics9030065.

[159] D. Gueners, H. Chanal, and B. C. Bouzgarrou, "Stiffness optimization of a cable driven parallel robot for additive manufacturing," in *Proc. IEEE Int. Conf. Robot. Automat. (ICRA)*, May 2020, pp. 843–849, doi: 10.1109/ICRA40945.2020.9197368.

[160] T. P. Tho and N. T. Thinh, "Using a cable-driven parallel robot with applications in 3D concrete printing," *Appl. Sci.*, vol. 11, no. 2, p. 563, Jan. 1, 2021, doi: 10.3390/app11020563.

[161] B. Zi, N. Wang, S. Qian, and K. Bao, "Design, stiffness analysis and experimental study of a cable-driven parallel 3D printer," *Mechanism Mach. Theory*, vol. 132, pp. 207–222, Feb. 2019, doi: 10.1016/j.mechmachtheory.2018.11.003.

[162] S. Abdelaziz, L. Barbé, P. Renaud, M. de Mathelin, and B. Bayle, "Control of cable-driven manipulators in the presence of friction," *Mechanism Mach. Theory*, vol. 107, pp. 139–147, Jan. 2017, doi: 10.1016/j.mechmachtheory.2016.09.014.

[163] P. H. Borgstrom *et al.*, "NIMS-PL: A cable-driven robot with self-calibration capabilities," *IEEE Trans. Robot.*, vol. 25, no. 5, pp. 1005–1015, Oct. 2009, doi: 10.1109/TRO.2009.2024792.

[164] E. Ida, D. Marian, and M. Carricato, "A deployable cable-driven parallel robot with large rotational capabilities for laser-scanning applications," *IEEE Robot. Automat. Lett*., vol. 5, no. 3, pp. 4140–4147, Jul. 2020, doi: 10.1109/LRA.2020.2989669.

[165] S. Seriani, P. Gallina, and A. Wedler, "A modular cable robot for inspection and light manipulation on celestial bodies," *Acta Astronaut. (U.K.)*, vol. 123, pp. 145–153, Jun. 2016, doi: 10.1016/j.actaastro.2016.03.020.

[166] Z. Shao, G. Xie, Z. Zhang, and L. Wang, "Design and analysis of the cable-driven parallel robot for cleaning exterior wall of buildings," *Int. J. Adv. Robot. Syst.*, vol. 18, no. 1, p. 172988142199031, Feb. 8, 2021, doi: 10.1177/1729881421990313.

[167] J. Izard, M. Gouttefarde, C. Baradat, D. Culla, and D. Sallé, "Integration of a parallel cable-driven robot on an existing building façade," in *Cable-Driven Parallel Robots*, T. Bruckmann and A. Pott, Eds. Cham, Switzerland: Springer-Verlag, 2012, pp. 149–164.

[168] L. Gagliardini, S. Caro, M. Gouttefarde, P. Wenger, and A. Girin, "A reconfigurable cable-driven parallel robot for sandblasting and painting of large structures," in *Proc. CableCon: Cable-Driven Parallel Robots*, Germany, 2014, pp. 275–291.

[169] N. Pedemonte *et al.*, "FASTKIT: A mobile cable-driven parallel robot for logistics," in *Advances in Robotics Research: From Lab to Market*, A. Grau, Y. Morel, A. Puig-Pey, and F. Cecchi, Eds. Cham, Switzerland: Springer-Verlag, 2019, pp. 141–163.

[170] C. Alias, I. Nikolaev, E. G. Correa Magallanes, and B. Noche, "An overview of warehousing applications based on cable robot technology in logistics," in *Proc. IEEE Int. Conf. Service Operations Logistics, and Informatics (SOLI)*, Singapore, Jul. 2018, pp. 232–239.

[171] E. Brau, F. Gosselin, and J. P. Lallemand, "Design of a singularity free architecture for cable driven haptic interfaces," in *Proc. 1st Joint Eurohaptics Conf. Symp. Haptic Interf. Virtual Environ. Teleoperator Syst. World Haptics Conf.*, Italy, 2005, pp. 208–213.

[172] M. M. Horoub, M. Hassan, and M. A. Hawwa, "Workspace analysis of a Gough-Stewart type cable marine platform subjected to harmonic water waves," *Mechanism Mach. Theory*, vol. 120, pp. 314–325, Feb. 2018, doi: 10.1016/j.mechmachtheory.2017.09.001.

[173] N. Y. Sergiienko, B. S. Cazzolato, B. Ding, and M. Arjomandi, "An optimal arrangement of mooring lines for the three-tether submerged point-absorbing wave energy converter," *Renew. Energy*, vol. 93, pp. 27–37, Aug. 2016, doi: 10.1016/j.renene.2016.02.048.

[174] F. Ben Abdallah, N. Azouz, L. Beji, S. Hima, and A. Abichou, "Modeling and control of an aerial robocrane using a wire driven system," in *Proc. Annu. American Control Conf. (ACC)*, USA, Jun. 2018, pp. 508–513.

[175] J. Erskine, A. Chriette, and S. Caro, "Wrench analysis of cable-suspended parallel robots actuated by quadrotor unmanned aerial vehicles," *J. Mechanisms Robot.*, vol. 11, no. 2, Apr. 1, 2019.

[176] J. Fink, N. Michael, S. Kim, and V. Kumar, "Planning and control for cooperative manipulation and transportation with aerial robots," *Int. J. Robot. Res.*, vol. 30, no. 3, pp. 324–334, Mar. 2011, doi: 10.1177/0278364910382803.

[177] F. Takemura, M. Enomoto, T. Tanaka, K. Denou, Y. Kobayashi, and S. Tadokoro, "Development of the balloon-cable driven robot for information collection from sky and proposal of the search strategy at a major disaster," in *Proc. IEEE/ASME Int. Conf. Adv. Intell. Mechatron.*, 2005, pp. 658–663, doi: 10.1109/AIM.2005.1511057.

[178] F. B. Abdallah, N. Azouz, L. Beji, and A. Abichou, "Modeling of a heavy-lift airship carrying a payload by a cable-driven parallel manipulator," *Int. J. Adv. Robot. Syst.*, vol. 16, no. 4, p. 172988141986176, Jul. 31, 2019, doi: 10.1177/1729881419861769.

[179] P. Arcara, L. D Stefano, S. Mattoccia, C. Melchiorri, and G. Vassura, "Perception of depth information by means of a wire-actuated haptic interface," in *Proc. IEEE Int. Conf. Robot. Automat.*, 2000, pp. 3443–3448, doi: 10.1109/ROBOT.2000.845258.

Mahmoud Zarebidoki, University of Auckland, Auckland, 1010, New Zealand. Email: mzar839@aucklanduni.ac.nz.

Jaspreet Singh Dhupia, University of Auckland, Auckland, 1010, New Zealand. Email: j.dhupia@auckland.ac.nz.

Weiliang Xu, University of Auckland, Auckland, 1010, New Zealand. Email: p.xu@auckland. ac.nz.